AD-A066 713 TEXAS INSTRUMENTS INC DALLAS EQUIPMENT GROUP F/G 17/10
SHORT-PERIOD NOISE ENVELOPE STATISTICS: A BASIS FOR ENVELOPE DE--ETC(U)
SEP 78 R UNGER F08606-77-C-0004
UNCLASSIFIED TI-ALEX(01)-TR-78-05 NL

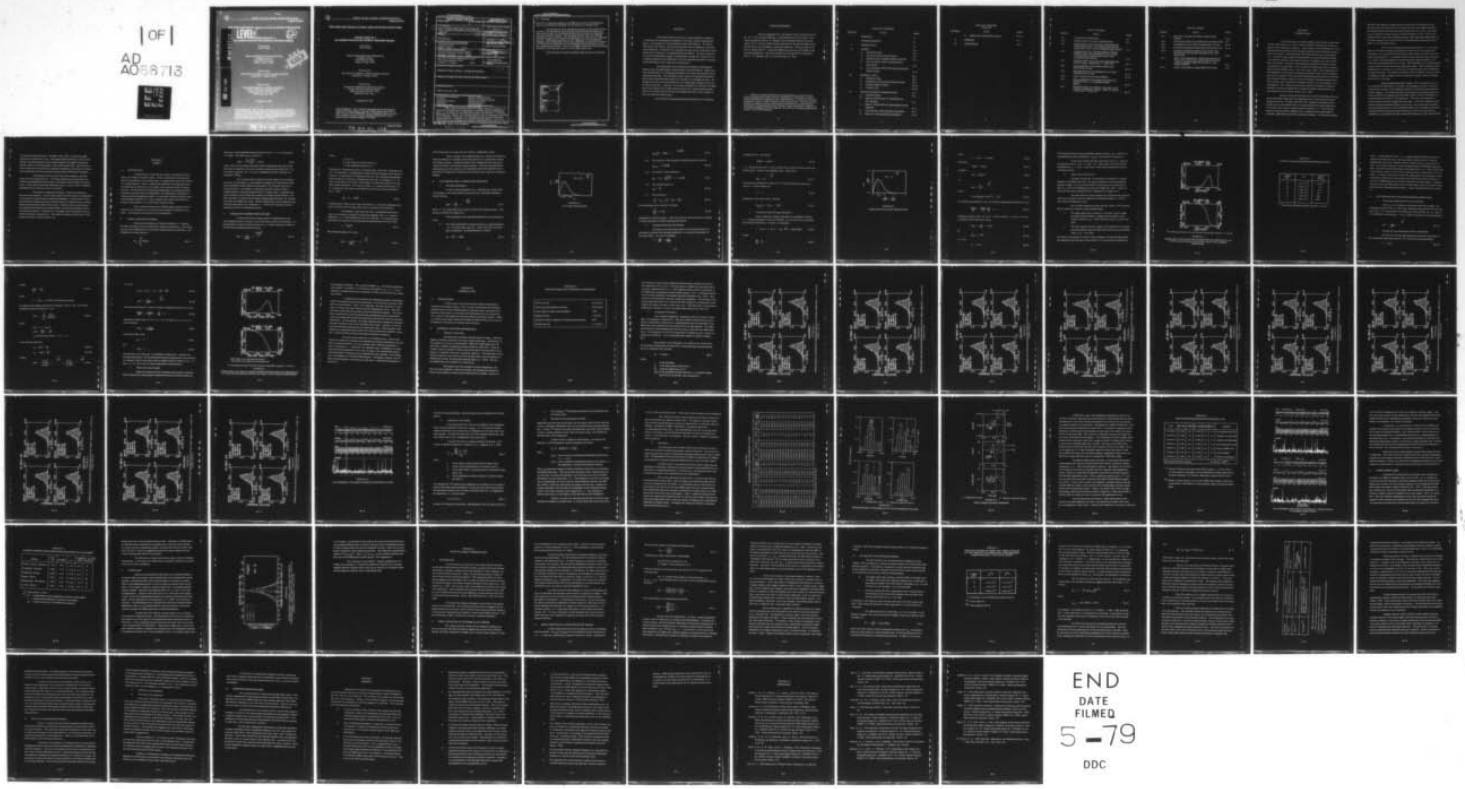

END
DATE FILMED
5-79
DDC

ALEX(01)-TR-78-06

SHORT-PERIOD NOISE ENVELOPE STATISTICS: A BASIS FOR ENVELOPE DETECTOR DESIGN

LEVEL II

12

TECHNICAL REPORT NO. 17

VELA NETWORK EVALUATION AND AUTOMATIC PROCESSING RESEARCH

Prepared by
Rudolf Unger

TEXAS INSTRUMENTS INCORPORATED
Equipment Group
Post Office Box 6015
Dallas, Texas 75222

Prepared for

AIR FORCE TECHNICAL APPLICATIONS CENTER
Alexandria, Virginia 22314

Sponsored by

ADVANCED RESEARCH PROJECTS AGENCY
Nuclear Monitoring Research Office
ARPA Program Code No. 7F10
ARPA Order No. 2551

26 September 1978

Acknowledgment. This research was supported by the Advanced Research Projects Agency, Nuclear Monitoring Research Office under Project VELA-UNIFORM, and accomplished under the technical direction of the Air Force Technical Applications Center under Contract Number F08606-77-C-0004.

ALEX(01)-TR-78-05

SHORT-PERIOD NOISE ENVELOPE STATISTICS: A BASIS FOR ENVELOPE DETECTOR DESIGN

TECHNICAL REPORT NO. 17
VELA NETWORK EVALUATION AND AUTOMATIC PROCESSING RESEARCH

Prepared by
Rudolf Unger

TEXAS INSTRUMENTS INCORPORATED
Equipment Group
Post Office Box 6015
Dallas, Texas 75222

Prepared for

AIR FORCE TECHNICAL APPLICATIONS CENTER
Alexandria, Virginia 22314

Sponsored by

ADVANCED RESEARCH PROJECTS AGENCY
Nuclear Monitoring Research Office
ARPA Program Code No. 7F10
ARPA Order No. 2551

26 September 1978

Acknowledgment: This research was supported by the Advanced Research Projects Agency, Nuclear Monitoring Research Office under Project VELA-UNIFORM, and accomplished under the technical direction of the Air Force Technical Applications Center under Contract Number F08606-77-C-0004.

UNCLASSIFIED

SECURITY CLASSIFICATION OF THIS PAGE (When Data Entered)

REPORT DOCUMENTATION PAGE	READ INSTRUCTIONS BEFORE COMPLETING FORM
1. REPORT NUMBER	2. GOVT ACCESSION NO. 3. RECIPIENT'S CATALOG NUMBER
4. TITLE (and Subtitle) (9) SHORT-PERIOD NOISE ENVELOPE STATISTICS: A BASIS FOR ENVELOPE DETECTOR DESIGN (14) TI	5. TYPE OF REPORT & PERIOD COVERED (9) Technical rept. no. 17
	6. PERFORMING ORG. REPORT NUMBER ALEX(01)-TR-78-05
7. AUTHOR(s) (10) Rudolf Unger	8. CONTRACT OR GRANT NUMBER(s) (15) F08606-77-C-0004, ARPA Order 2551
9. PERFORMING ORGANIZATION NAME AND ADDRESS Texas Instruments Incorporated Equipment Group Dallas, Texas 75222	10. PROGRAM ELEMENT, PROJECT, TASK AREA & WORK UNIT NUMBERS VELA T/8705/B/PMP
11. CONTROLLING OFFICE NAME AND ADDRESS Advanced Research Projects Agency Nuclear Monitoring Research Office Arlington, Virginia 22209	(11) 12. REPORT DATE 26 September 1978
	13. NUMBER OF PAGES 78
14. MONITORING AGENCY NAME & ADDRESS (if different from Controlling Office) Air Force Technical Applications Center VELA Seismological Center Alexandria, Virginia 22314	15. SECURITY CLASS. (of this report) UNCLASSIFIED
	15a. DECLASSIFICATION/DOWNGRADING SCHEDULE

16. DISTRIBUTION STATEMENT (of this Report)

APPROVED FOR PUBLIC RELEASE, DISTRIBUTION UNLIMITED

(12) 78p.

17. DISTRIBUTION STATEMENT (of the abstract entered in Block 20, if different from Report)

18. SUPPLEMENTARY NOTES

ARPA Order No. 2551

19. KEY WORDS (Continue on reverse side if necessary and identify by block number)

Instantaneous amplitude	Seismic signal detection
Envelope	Seismic surveillance system
Instantaneous power	Envelope detection
Detection	Power detection
False alarm rate	Controlled false alarm rate

20. ABSTRACT (Continue on reverse side if necessary and identify by block number)

This report focuses on the use of certain detection statistics, in particular the instantaneous amplitude or envelope, and the instantaneous power, in the design of a controlled false alarm rate detector. To achieve false alarm rate control, the detection statistic must be stationary, but need not be Gaussian. Parameters of a Gaussian process can be conveniently transformed into a stationary, normalized detection statistic. For an envelope detector the normalization consists of dividing the envelope by a long-

Power

DD FORM 1 JAN 73 1473 EDITION OF 1 NOV 65 IS OBSOLETE

UNCLASSIFIED

SECURITY CLASSIFICATION OF THIS PAGE (When Data Entered)

JOB

405 076

20. continued

term (1 to 2 minutes) estimate of the RMS noise level; the instantaneous power is normalized by dividing it by the long-term average power.

The stationarity of the normalized envelope is demonstrated with one hour of uninterrupted, Korean Seismic Research Station single-site, short-period noise, by compiling distributions of the base-ten logarithm of the normalized envelope. The envelopes closely follow the Rayleigh distribution which is the theoretical distribution for envelopes of a Gaussian process. Retaining this model at the 5% significance level establishes adequate control of the false alarm rate. Typically, an envelope threshold of 12 dB above the RMS noise level should yield 13 false alarms per hour for a single detection trial. The use of multiple detection trials and multiple detection criteria should result in a lower false alarm rate.

Various detector design optimization approaches are discussed.

ABSTRACT

This report focuses on the use of certain detection statistics, in particular the instantaneous amplitude or envelope, and the instantaneous power, in the design of a controlled false alarm rate detector. To achieve false alarm rate control, the detection statistic must be stationary, but need not be Gaussian. Parameters of a Gaussian process can be conveniently transformed into a stationary, normalized detection statistic. For an envelope detector the normalization consists of dividing the envelope by a long-term (1 to 2 minutes) estimate of the RMS noise level; the instantaneous power is normalized by dividing it by the long-term average power.

The stationarity of the normalized envelope is demonstrated with one hour of uninterrupted, Korean Seismic Research Station single-site, short-period noise, by compiling distributions of the base-ten logarithm of the normalized envelope. The envelopes closely follow the Rayleigh distribution which is the theoretical distribution for envelopes of a Gaussian process. Retaining this model at the 5% significance level establishes adequate control of the false alarm rate. Typically, an envelope threshold of 12 dB above the RMS noise level should yield 13 false alarms per hour for a single detection trial. The use of multiple detection trials and multiple detection criteria should result in a lower false alarm rate.

Various detector design optimization approaches are discussed.

ACKNOWLEDGMENTS

Various suggestions by, and frequent critical discussions with Dr. R. L. Sax, Program Manager, contributed greatly to this study. Personal discussions with Dr. F. Ringdal of the Norwegian Research Council, and Dr. R. T. Lacoss of MIT Lincoln Laboratories clarified possible causes of false alarm rate instability in automatic detectors. Software support by Ms. K. Wilson and D. G. Black III enabled the production and display of the envelope histograms. The text and figures were prepared for printing by Mrs. C. B. Saunders, Ms. S. Jacobs and Ms. B. Olson.

TABLE OF CONTENTS

TABLE OF CONTENTS
(continued)

LIST OF FIGURES

LIST OF TABLES

SECTION I
INTRODUCTION

In the concept of a world-wide seismic surveillance system such as described by Sax et al. (1974), reliable automatic detection and timing of seismic event signals are essential. If the system is to be optimized for event detection then the effects of missed signals and false alarm detections must be taken into account. The false alarm rate (FAR) must be made controllable, i.e., it must be made constant and predictable for a given threshold setting of the detection statistic, and should be as low as possible for a given probability of detection. Inversely, the probability of detection should be as high as possible for a given FAR. This is a general requirement of any communication system (Schwartz et al., 1966; Van Trees, 1968). This requirement is also applicable to the seismic surveillance problem in that P-wave transmissions from a seismic event convey the timing information needed to locate and time transient seismic events, to edit time windows containing signals associated with the event, and finally to identify the source as an earthquake or as an explosion. For a seismic surveillance system, an example of optimum threshold control was worked out in a study on feedback and parameter update aspects in such a system (Unger et al., 1974).

Several recent developments were aimed at providing front-end short-period (SP) signal detection algorithms which could satisfy the above mentioned criteria. Swindell and Snell (1977) designed an automatic power detector with a controllable FAR, by transforming the detector output into a zero-mean, unit-variance normal random variable (r.v.). At the Korean Seismic Research Station (KSRS) array, a comparison was made between automatic signal detections and an analyst's detections. The results indicated

that 90% of the analyst's signal picks were detected if the threshold of the automatic detector was set at 8.4 dB signal-to-noise ratio (SNR) and 50% of the analyst's picks were detected with a threshold set at 9.6 dB. These figures are based on a fixed variance of the noise power of 3 dB. The corresponding FAR for these two threshold settings, when employing eight beams, is 25 false alarms per hour (FA/H) at the 8.4 dB threshold setting and 4 FA/H at the 9.6 dB threshold setting.

The receiver operating characteristics (ROC), i.e., the probability of detection versus the probability of false alarm (or the FAR) characteristics, can be improved by processors which enhance the SNR of the detector input waveform. An example of such a processor for array waveforms is a recently improved adaptive beamforming (ABF) algorithm (Shen, 1977, 1978) with typical SNR gains of 5 to 10 dB. This algorithm can be implemented in front-end processors such as the station processor. Other methods of SNR enhancement, of course, are various forms of pre-filtering such as bandpass or Wiener filtering. The problem with these latter methods is, however, that if designed to apply to signals of diverse spectral contents, their processing gain cannot be very high.

Another, independent effort (Unger, 1978) evaluated the use of the instantaneous amplitude or envelope, the instantaneous phase, and the instantaneous frequency in the automatic detection, timing and measurement of seismic signals. This study resulted in the design of an automatic phase detector and timer for long-period (LP) surface waves, and of an automatic envelope detector and timer for SP bodywaves. The latter was designed to closely follow an analyst's signal detection logic. An initial evaluation of this detector showed promising results: for a given, but not necessarily typical, set of Norwegian Seismic Array (NORSAR) single-site recordings of Eurasian earthquake and presumed explosion waveforms, the SP envelope detector, operating at a peak-signal-to-peak-noise ratio threshold of 3 dB, detected 69%

of 16 signals having less than 12 dB SNR, with a FAR of 7 FA/H; the RMS timing error was about 0.2 sec. Remaining technical problem areas for this detector are detecting and timing emergent signals and signals interfering with the coda of a preceding signal, and controlling the FAR. The solution of these problems must precede any extensive evaluation of the detector to determine realistically its full operating characteristics and detection capability.

This report focuses on one of the above problems, the FAR control of the envelope detector. The study analytically and empirically describes the probability density function of envelope measurements of seismic noise. If the model fits the data sufficiently close, it can be used to establish algorithms for the efficient control of the FAR.

The report is organized as follows. Section II contains our theoretical development. We first show briefly how FAR control is established in principle for a given detection statistic distribution. We then derive normalized detection statistics and their distributions for a Gaussian noise process, and describe how these enable FAR control. In Section III we present empirically gathered distributions and observations, and test the goodness-of-fit of our theoretical models. In Section IV, we interpret this information in terms of detector design considerations. The study is summarized in Section V and related literature is listed in Section VI.

SECTION II
THEORY

A. INTRCDUCTICN

In this section, we describe the control of a detector's false alarm rate (FAR) for Gaussian noise. First, we describe the general problem of maintaining, in an average sense, a constant false alarm rate (CFAR) for a signal detector. Next, we discuss the problem of normalizing a time-varying Gaussian process to a zero-mean, unit-variance or N(0, 1) normal process. We then derive the normalized distribution of two signal detection parameters and their base-ten logarithms: the instantaneous amplitude or envelope and the instantaneous power. In each case we show how these normalized random variables (r. v.) may be used in the control of the FAR of a seismic signal detector, for a given noise frequency band.

For an excellent summary of related tutorial material and an extensive list of literature, we refer to the first chapter of Schwartz et al. (1966). This material is the basis for our development.

B. FALSE ALARM RATE CONTROL

If the noise distribution of a detection statistic, x, is known, the FAR of a detector can be controlled by setting a threshold x_T. For values $x>x_T$ the noise hypothesis is rejected and a signal detection is declared. The probability of a false alarm is

$$P_F = \int_{x_T}^{\infty} p(x)dx, \qquad \text{(II-1)}$$

where p(x) is the probability density function of the r.v., x, in the absence of a signal. The false alarm rate then is

$$FAR = \frac{P_F \cdot 3600}{\Delta T} \quad FA/H \tag{II-2}$$

where ΔT is the interval (in seconds) between independent detection trials. This interval depends on the noise frequency band (Sections III and IV). For our study we assume $\Delta T = 0.36$ sec; in Equation (II-2) the FAR then corresponds to $10^4 P_F$.

If a constant FAR is required to detect signals in non-stationary noise, the threshold x_T must adapt to changes in the parameters of the noise probability density function and therefore, the threshold will have to change with time. In contrast, a stationary detection statistic yields a constant FAR for a given threshold setting. In many cases, a stationary detection statistic can be obtained by means of a suitable transformation. It is also convenient to express the threshold settings logarithmically, for instance in dB above the RMS noise value. These transformations are discussed in the following subsections, for a Gaussian r.v., and for the envelope and the instantaneous power of a Gaussian process.

C. NORMALIZED GAUSSIAN NOISE PROCESS

If noise stems from a large number of independent (or non-interacting) particles or sources, the noise process tends to be Gaussian, i.e., the parameters involved in this process are r.v. whose variation is ruled by the Gaussian probability density function:

$$p(x) = \frac{1}{\sqrt{2\pi}\sigma} \; e^{-\frac{(x-\mu)^2}{2\sigma^2}} \tag{II-3}$$

where

x is a r.v.

μ is the mean or average value of x

σ is the standard deviation of x.

Examples of a Gaussian process are thermal noise, shot noise, Brownian motion. In seismology, if instantaneous random pressure changes in the earth are caused by a large number of independent sources, the resulting seismograms show waveforms in which the instantaneous value n(t) is a Gaussian r.v. Results of this nature were found, among others, by Sax (1965); this article also lists related literature. The variance of this r.v. equals the total power N, or, equivalently, the square of the RMS level of zero-mean noise (Schwartz et al., 1966):

$$\sigma_n^2 = N = RMS^2 \quad . \tag{II-4}$$

In Equation (II-3) both μ and σ may vary with time. In noise seismograms the mean is usually zero; the total noise power in general varies with time.

In designing a signal detector with a controllable false alarm rate it is desirable to transform the detection statistic into a r.v. which is stationary, i.e., whose statistics do not vary with time. In a Gaussian process this can be achieved by performing the transformation (Lacoss, 1972):

$$z = \frac{x - \mu}{\sigma} \quad . \tag{II-5}$$

This changes Equation (II-3) into:

$$p(z) = \frac{1}{\sqrt{2\pi}} \; e^{-\frac{z^2}{2}} \tag{II-6}$$

which always has zero mean and unit variance, independent of time.

This z-statistic was adopted by Sax et al. (1974) as a preferred detection statistic for automatic front-end detection in a world-wide seismic surveillance system. Swindell and Snell (1977) implemented this concept to control the FAR of an automatic power detector. This was accomplished by transforming the time-varying, near-Gaussian distributed logarithm of the short-term average power (log STA) in this manner into a stationary detection statistic.

D. FAR CONTROL WITH A NORMALIZED ENVELOPE

1. Envelope Distribution

It can be shown (Schwartz et al., 1966) that the envelope R(t) of a Gaussian, zero-mean random process n(t) has a Rayleigh probability density function:

$$p(R) = \frac{R}{N} e^{-\frac{R^2}{2N}} \qquad \text{(II-7)}$$

where $N = \sigma_n^2$ is the total noise power over the noise frequency band. This function is sketched in Figure II-1.

Some properties of the Rayleigh distribution are summarized below:

(i) The entire distribution is characterized by a single parameter, i. e., the most likely value R_ℓ. This is the value for which p(R) is maximum. By differentiation we obtain:

$$R_\ell = \sqrt{N} = \text{RMS} \qquad \text{(II-8)}$$

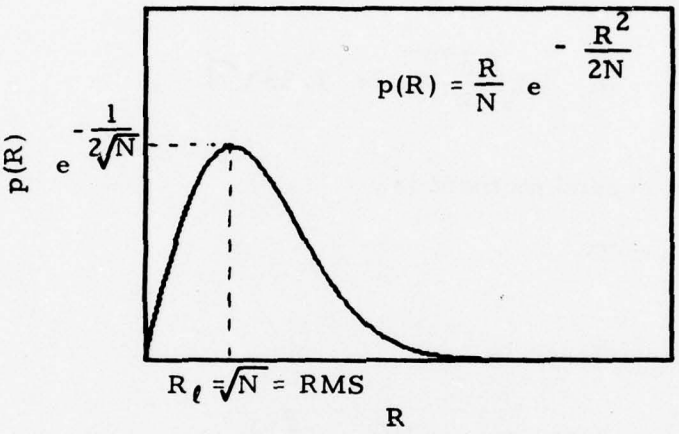

FIGURE II-1

RAYLEIGH DISTRIBUTION

$$p_{max}(R) = p(R_\ell) = e^{-1/(2\sqrt{N})} \quad . \tag{II-9}$$

(ii) The median or 50% cumulative distribution point occurs at

$$R_{med} = 1.185\sqrt{N} \quad . \tag{II-10}$$

(iii) The mean or first moment is

$$\mu_R = m_1 = \sqrt{\frac{\pi}{2}N} = 1.25\sqrt{N} \quad . \tag{II-11}$$

(iv) The second moment is

$$m_2 = 2N \quad . \tag{II-12}$$

(v) The variance is

$$\sigma_R^2 = m_2 - m_1^2 = N(2 - \frac{\pi}{2}) \quad . \tag{II-13}$$

From Equations (II-11) and (II-13) follows

$$\frac{\sigma_R}{\mu_R} = 0.525 \quad , \tag{II-14}$$

independent of the noise power. This value may be used to test if the envelope of a given waveform is indeed Rayleigh-distributed.

2. Normalized Envelope Distribution

To enable convenient FAR control of an envelope detector we proceed to normalize the Rayleigh distribution by making it independent of the noise power. For this we substitute

$$u = \frac{R}{\sqrt{N}} = \frac{R}{RMS} \tag{II-15}$$

in Equation (II-7), and require

$$p(R)dR = p(u)du \quad , \tag{II-16}$$

i. e., the probability that R has a certain value must be the same as the probability that u has the corresponding value. This yields

$$p(u) = ue^{-\frac{u^2}{2}} \quad . \tag{II-17}$$

This function is sketched in Figure II-2. We observe that the most likely value of u always equals one:

$$u_\ell = 1 \quad , \tag{II-18}$$

independent of the noise power, and that

$$p_{max}(u) = p(u_\ell) = 1/\sqrt{e} \quad . \tag{II-19}$$

3. Normalized Log-Envelope Distribution

Since a detector is usually operated in a logarithmic fashion, i. e., setting thresholds in terms of dB SNR, we now derive the normalized log-envelope distribution. For this, we substitute

$$y = \log u = \log R - \log \sqrt{N} = \log(R/RMS) \tag{II-20}$$

so that

$$\frac{dy}{du} = \frac{k}{u} \quad , \tag{II-21}$$

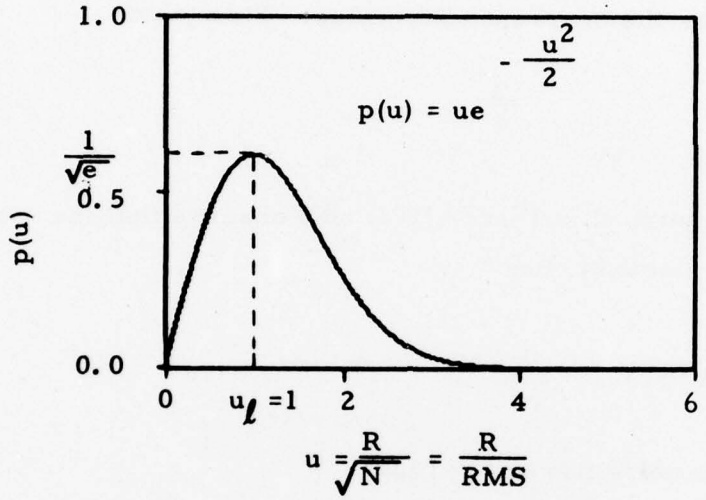

FIGURE II-2

NORMALIZED RAYLEIGH DISTRIBUTION

where

$$k = \log e = 0.43429 \quad . \tag{II-22}$$

Requiring

$$p(y)dy = p(u)du \tag{II-23}$$

we obtain

$$p(y) = \frac{u}{k} p(u) \tag{II-24}$$

or

$$p(y) = \frac{u^2}{k} e^{-\frac{u^2}{2}} \quad , \tag{II-25}$$

where

$$u \equiv \text{antilog}(y) \equiv \log^{-1} y = 10^y. \tag{II-26}$$

The maxima and minima of $p(y)$ are found by equating the derivative to zero:

$$\frac{dp(y)}{dy} = \frac{dp(y)}{du} \frac{du}{dy} = 0 \quad , \tag{II-27}$$

resulting in minima $p(y) \rightarrow 0$ for $y \rightarrow -\infty$ $(u = 0)$ and $y \rightarrow +\infty$ $(u \rightarrow +\infty)$, and a maximum at the most likely value:

$$p(y_\ell) = \frac{2}{ke} = 1.694 \tag{II-28}$$

for

$$u(y_\ell) = \sqrt{2} \quad , \tag{II-29}$$

i. e., for

$$y_\ell = 0.15 \quad . \tag{II-30}$$

The normalized log-envelope probability density function $p(y)$, and the corresponding false alarm probability $P_F(y_T)$ are sketched in Figure II-3.

It may seem strange that the most likely value of y does not correspond to that of u ($u_\ell = 1$; $y(u_\ell) = 0$). This is due to the fact that the transformation $y = \log u$ is non-linear, which shows particularly clearly in Equation (II-24).

4. False Alarm Rate Control

The above shows that, by dividing the envelope by a running estimate of the RMS noise level, we obtain a stationary envelope detection statistic R/RMS. For any desired FAR we then can set an envelope threshold R_T at the corresponding level above the RMS noise value. Table II-1 lists the FAR values computed for the righthand tail of Figure II-3.

The table shows that for envelopes of a Gaussian noise process, relatively low FAR values are obtained for threshold settings of 12 dB or more above the RMS noise level.

Our recently designed envelope detector (Unger, 1978) requires that two detection criteria be met simultaneously:

- The signal-plus-noise envelope in a test gate of given length must exceed the maximum, lagging noise envelope a given number of times (e. g., 10% to 30% of the time in a 4-sec test gate)
- The ratio between the first 'signal' envelope peak in a test gate and the maximum noise envelope must exceed a given threshold value (e. g., 2 or 3 dB).

We observe from Figure II-3 that, if the envelopes are Rayleigh-distributed, the maximum noise envelope is most likely 10 to 12 dB above the RMS noise

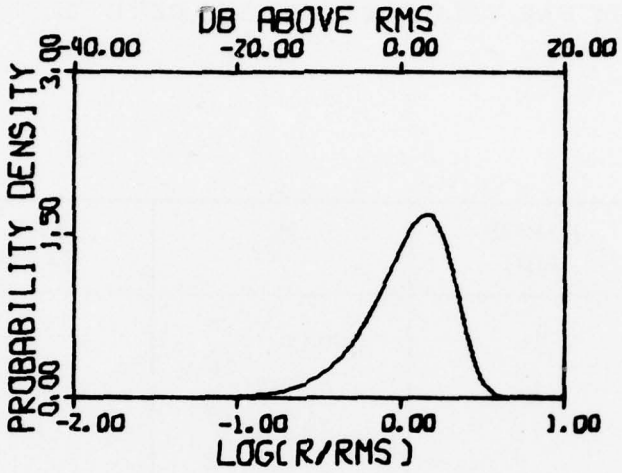

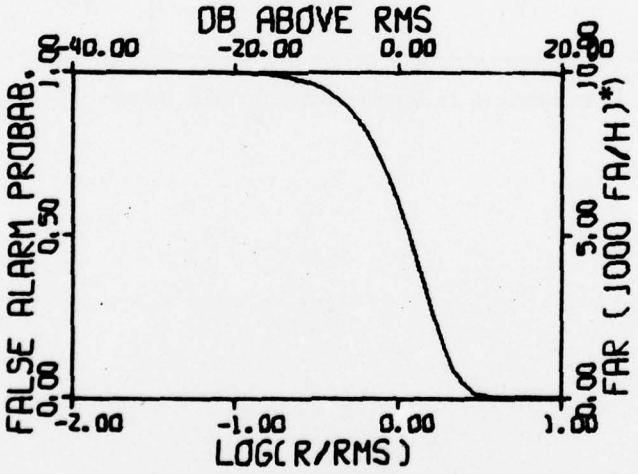

*) assuming minimum interval between independent samples = 0.36 sec

FIGURE II-3

NORMALIZED LOG-ENVELOPE DISTRIBUTION AND PROBABILITY OF FALSE ALARM (SINGLE DETECTION TRIAL) FOR GAUSSIAN NOISE MODEL

TABLE II-1

LOW FAR VALUES FOR SINGLE DETECTION TRIALS

R/RMS (dB)	P_F	FAR*) (FA/H)
16	2.00×10^{-8}	2×10^{-4}
14	2.00×10^{-5}	0.2
12	1.34×10^{-3}	13.4
10	1.69×10^{-2}	169
8	7.88×10^{-2}	788
6	2.04×10^{-1}	2040

*) Assuming independent-sample interval = 0.36 sec.

value. A single detection trial, i. e., requiring that the maximum noise envelope is exceeded only once, then would give a FAR of 169 to 13.4 FA/H. Multiple detection trials, together with the second criterion, will reduce the FAR. In an initial evaluation of this envelope detector on NORSAR single-site data, varying the threshold settings as indicated above, i.e., 10% to 30% for the first criterion, and 2 to 3 dB for the second criterion, yielded FARs of 7 to 20 FA/H. As will be described in Section III, applying the envelope detector with thresholds of 30% for the first criterion and 3 dB for the second criterion to one hour of KSRS single-site noise data resulted in one false alarm. Considerably more noise and signal data need to be processed to more accurately assess this detector's operating characteristics. This is discussed further in Section IV.

E. FAR CONTROL WITH THE INSTANTANEOUS NOISE POWER

1. Normalized Instantaneous-Noise Distribution

Below, we will consider an alternative detection statistic, the instantaneous power $n^2(t)$ of a zero-mean, Gaussian noise process n(t) with total power $\sigma_n^2 = N$. As described in the first part of this section, the r.v. n(t) can be normalized by substituting $v = n/\sigma_n$ to obtain a stationary N(0, 1) distribution:

$$p(v) = \frac{1}{\sqrt{2\pi}} e^{-\frac{v^2}{2}} . \qquad \text{(II-31)}$$

2. Normalized Log-Instantaneous-Power Distribution

We now will study the distribution of the base-ten logarithm of the normalized instantaneous power $v^2(t)$, and make the transformation

$$w = \log v^2 \qquad \text{(II-32)}$$

so that

$$\frac{dw}{dv} = \frac{2k}{v} \tag{II-33}$$

where

$k = \log e = 0.43429$ as defined previously.

According to the fundamental theorem (Papoulis, 1965; p. 126), we find the probability density function for w by

$$p(w) = \sum_{i=1}^{n} \frac{p(v_i)}{|g'(v_i)|} \tag{II-34}$$

where

$$g(v) = w = \log v^2$$

$$g'(v) = \frac{dw}{dv} = \frac{2k}{v}$$

v_i are the roots of $g(v)$, $i = 1, 2, \ldots, n$.

In our case the roots are

$$v_1 = \log^{-1} \frac{w}{2} \tag{II-35a}$$

$$v_2 = -\log^{-1} \frac{w}{2} \tag{II-35b}$$

so that

$$p(w) = \frac{|v_1|}{2k\sqrt{2\pi}} e^{-\frac{v_1^2}{2}} + \frac{|v_2|}{2k\sqrt{2\pi}} e^{-\frac{v_2^2}{2}} \tag{II-36}$$

or, since

$$|v_1| = |v_2| = v_1 = \log^{-1} \frac{w}{2} \quad , \tag{II-37}$$

$$p(w) = \frac{v_1}{k\sqrt{2\pi}} e^{-\frac{v_1^2}{2}} \quad . \tag{II-38}$$

The maxima and minima of p(w) are found by equating its derivative to zero:

$$\frac{dp(w)}{dw} = \frac{dp(w)}{dv} \cdot \frac{dv}{dw} = 0 \quad , \tag{II-39}$$

resulting in minima $p(w) \rightarrow 0$ for $w \rightarrow -\infty$ $(v = 0)$ and for $w \rightarrow +\infty$ $(v \rightarrow +\infty)$, and a maximum

$$p(w_\ell) = \frac{1}{k\sqrt{2\pi e}} \tag{II-40}$$

at the most likely value

$$w_\ell = 0 \quad , \tag{II-41}$$

for

$$v(w_\ell) = 1 \quad . \tag{II-42}$$

The functions p(w) and $P_F(w)$ are sketched in Figure II-4. Like the log-envelope distribution, the log-instantaneous-power distribution is non-symmetric (skewed), and its most likely value is shifted relative to that of v ($v_\ell = 0$; $w(v_\ell) \rightarrow -\infty$), due to the non-linear logarithmic transformation.

3. False Alarm Rate Control

Figure II-4 shows that for a Gaussian noise process a desired FAR is obtained by controlling the instantaneous-power threshold relative to

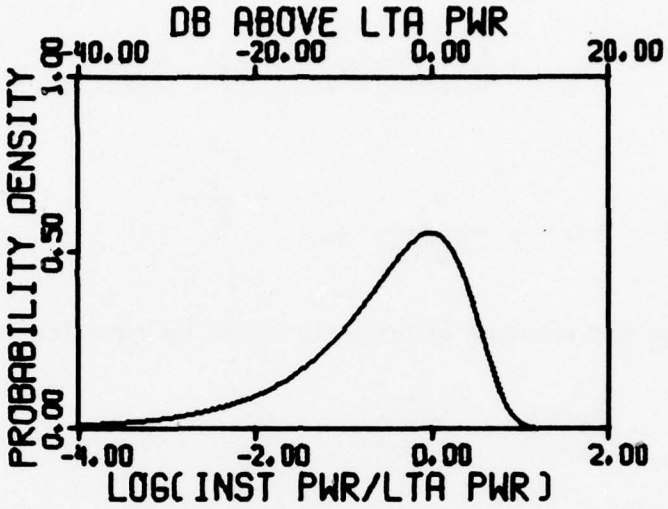

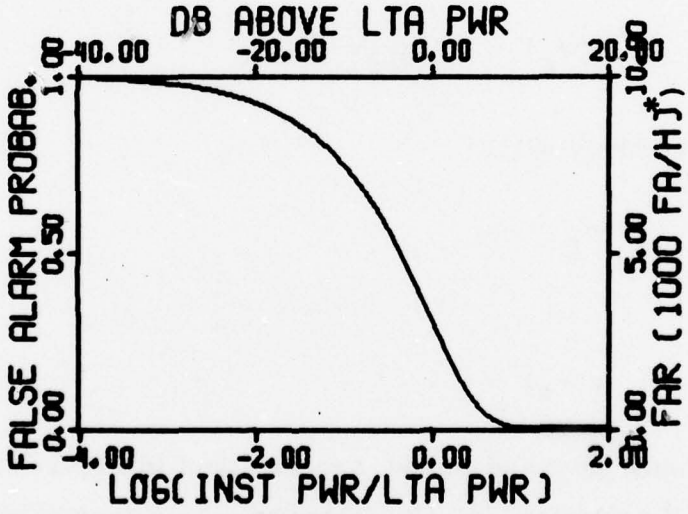

INST PWR is the instantaneous power
LTA PWR is the long-term average power

*) Assuming minimum interval between independent samples = 0.36 sec

FIGURE II-4

NORMALIZED LOG-INSTANTANEOUS-POWER DISTRIBUTION AND PROBABILITY OF FALSE ALARM (SINGLE DETECTION TRIAL) FOR GAUSSIAN NOISE MODEL

the average noise power. For a given threshold w_T, the FAR is predictable and constant. Low FAR's (< 10 FA/H) are obtained for $w_T = 1.1$, corresponding to instantaneous-power thresholds of 11 dB or more above the average noise power.

Comparing the normalized log-instantaneous-power distribution with the normalized log-envelope distribution, we note that the variance of the latter is much smaller. This is to be expected, since the envelope of a waveform, of course, has less variation than its instantaneous value. This characteristic could make the envelope a preferred detection statistic. We further observe that the tail of the normalized log-instantaneous-power distribution rises less sharply with decreasing values than does the tail of the log-envelope distribution. At first thought, one might interpret this as though the instantaneous power would provide a more favorable FAR control. However, we do not know the parameter distributions for signal-plus-noise. Determination of the difference in operating characteristics for these two detection statistics, therefore, requires further analysis and probably empirical evaluation.

We have demonstrated that, for Gaussian noise, control of the FAR can be effectively obtained with instantaneous detection parameters derived from a Gaussian process. It is not necessary that a detection parameter itself is a Gaussian r.v. Therefore, for Gaussian noise, averaging of an instantaneous detection parameter such as the envelope or the instantaneous power, with the purpose of obtaining a near-Gaussian detection statistic, is not mandatory in the design of a controlled FAR detector. Averaging, however, may enhance the performance of a detector in other ways. This will be discussed in Section IV.

SECTION III
EMPIRICAL DATA

A. INTRODUCTION

In this section we discuss detection statistic distributions compiled from empirical data. First, we show log-envelope distributions obtained from one hour of KSRS single-site SP noise data, and discuss the goodness-of-fit relative to the theoretical distribution derived in Section II. These data are then augmented with observations previously reported. Next, we consider power data obtained by Swindell and Snell (1977) in the course of designing and evaluating an automatic power detector.

B. EMPIRICAL ENVELOPE DISTRIBUTIONS

1. Histogram Generation

The previously mentioned envelope detector (Unger, 1978) was adapted to handle consecutive records as uninterrupted data. In this form, it was applied to one hour of uninterrupted, unfiltered, KSRS single-site, SP noise data, using the operating parameters listed in Table III-1. These parameter values are similar to those used in the initial envelope detector evaluation, as reported in the above mentioned reference. The parameter values listed in Table III-1 are also in use at the present time in the evaluation of a multivariate seismic discrimination package (Sax et al., 1978). The one-hour KSRS noise test resulted in one false alarm.

The program was also adapted to produce histograms, for 102.4-sec data segments, of the log-envelope, the instantaneous frequency and the mean frequency, using various sample-interval lengths. Below, we

TABLE III-1

ENVELOPE DETECTOR OPERATING PARAMETERS

Warm-up time	:	60 seconds
Peak-noise tapering time constant	:	180 seconds
Peak-signal-to-peak-noise threshold	:	3 dB
Signal test gate	:	4 seconds
Required relative frequency of detections in test gate	:	30%
Sample interval	:	0.1 second

will analyze the log-envelope histograms obtained from sampling consecutive data segments every 0.4 sec. The combination of KSRS noise spectrum and instrument response (Prahl et al., 1975) suggests that the effective bandwidth of the KSRS noise seismograms approximately equals 2.5 Hz. A sampling interval of 0.4 sec then should give independent samples (Schwartz et al., 1966). This results in 256 independent envelope samples per histogram. The transfer of detection parameters from one record to the next requires an overlap equal to the length of the signal test gate, in this case 4 sec. The start times of consecutive histograms, therefore, are 98.4 sec apart rather than the full 102.4 sec.

2. Histogram Presentation

The resulting histograms, reflecting a total of one hour of noise data, are presented in Figure III-1. The log-envelope values have been normalized, as described in Section II, by subtracting the base-ten logarithm of the RMS noise level measured over the entire 102.4-sec data segment. The upper axis shows the corresponding noise envelope values in dB above the RMS noise level. The histogram at 11:52:12.0 (Figure III-1) contains the only 'alarm' reported by the detector. The corresponding data segment is shown in Figure III-2.

Also plotted in each histogram, as a solid curve, are the relative frequencies found from the theoretical, normalized log-envelope distribution for a Gaussian noise process:

$$p_i = \Delta y \, p(y_i) \, , \qquad \text{(III-1)}$$

where

- i is the bin index,
- y_i is the value at the center of bin i ,
- Δy is the bin width (here = 0.1),
- $p(y_i)$ is the probability density value for y_i as given by Equations (II-25) and (II-26), and in Figure II-3.

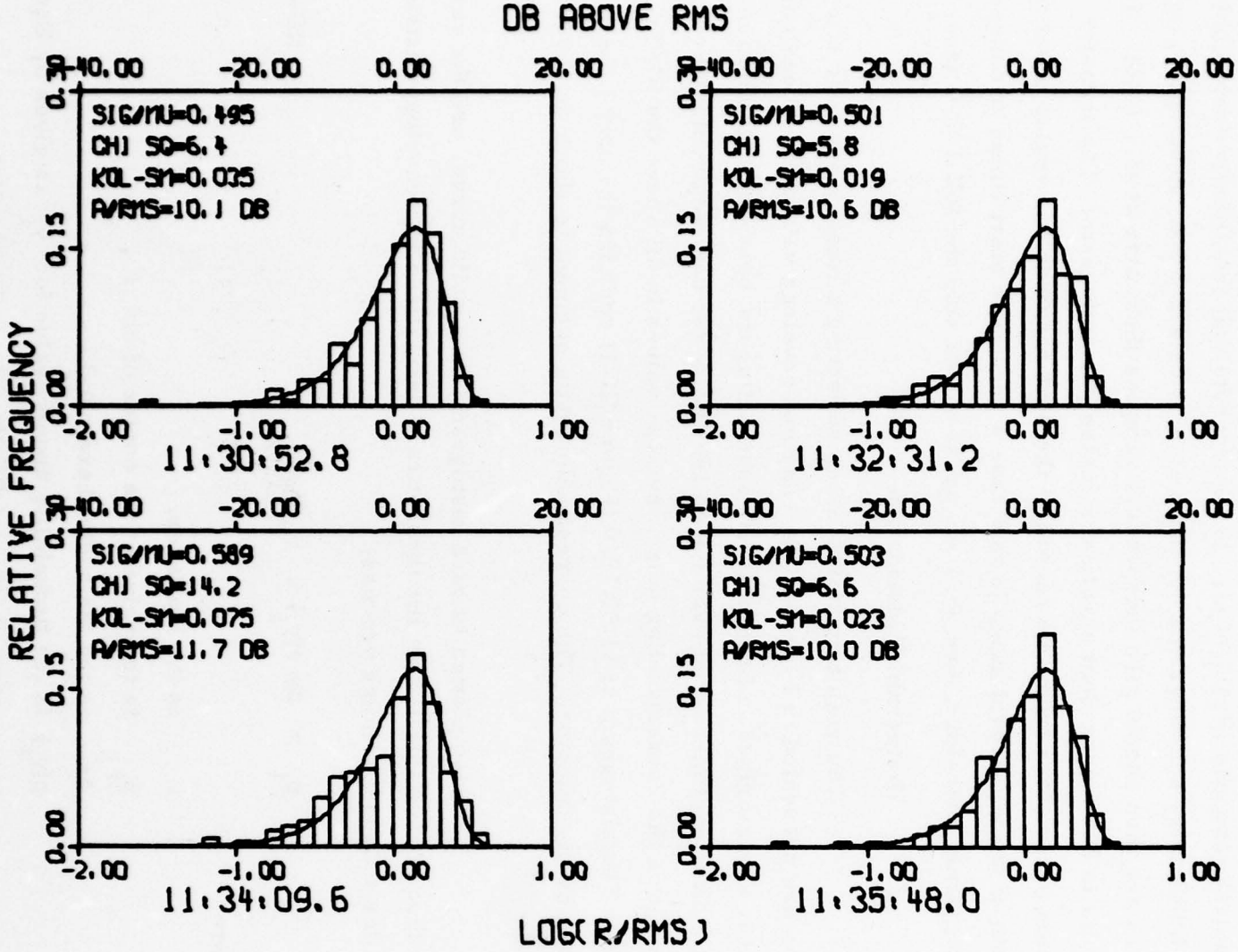

FIGURE III-1

NORMALIZED LOG-ENVELOPE DISTRIBUTIONS FOR SP NOISE, KSRS SITE 1, 9 JUNE 1976
(PAGE 1 OF 10)

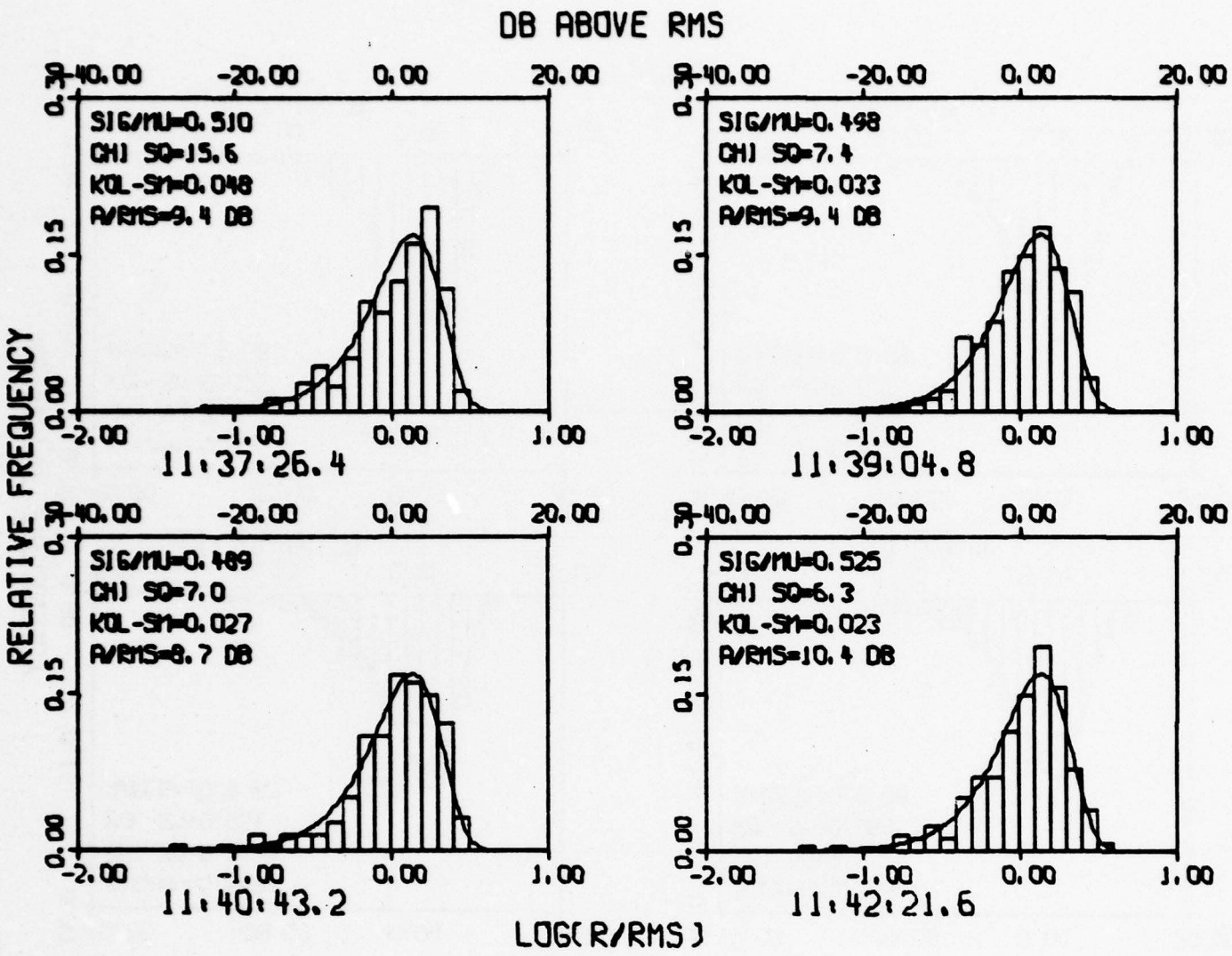

FIGURE III-1

NORMALIZED LOG-ENVELOPE DISTRIBUTIONS FOR SP NOISE, KSRS SITE 1, 9 JUNE 1976
(PAGE 2 OF 10)

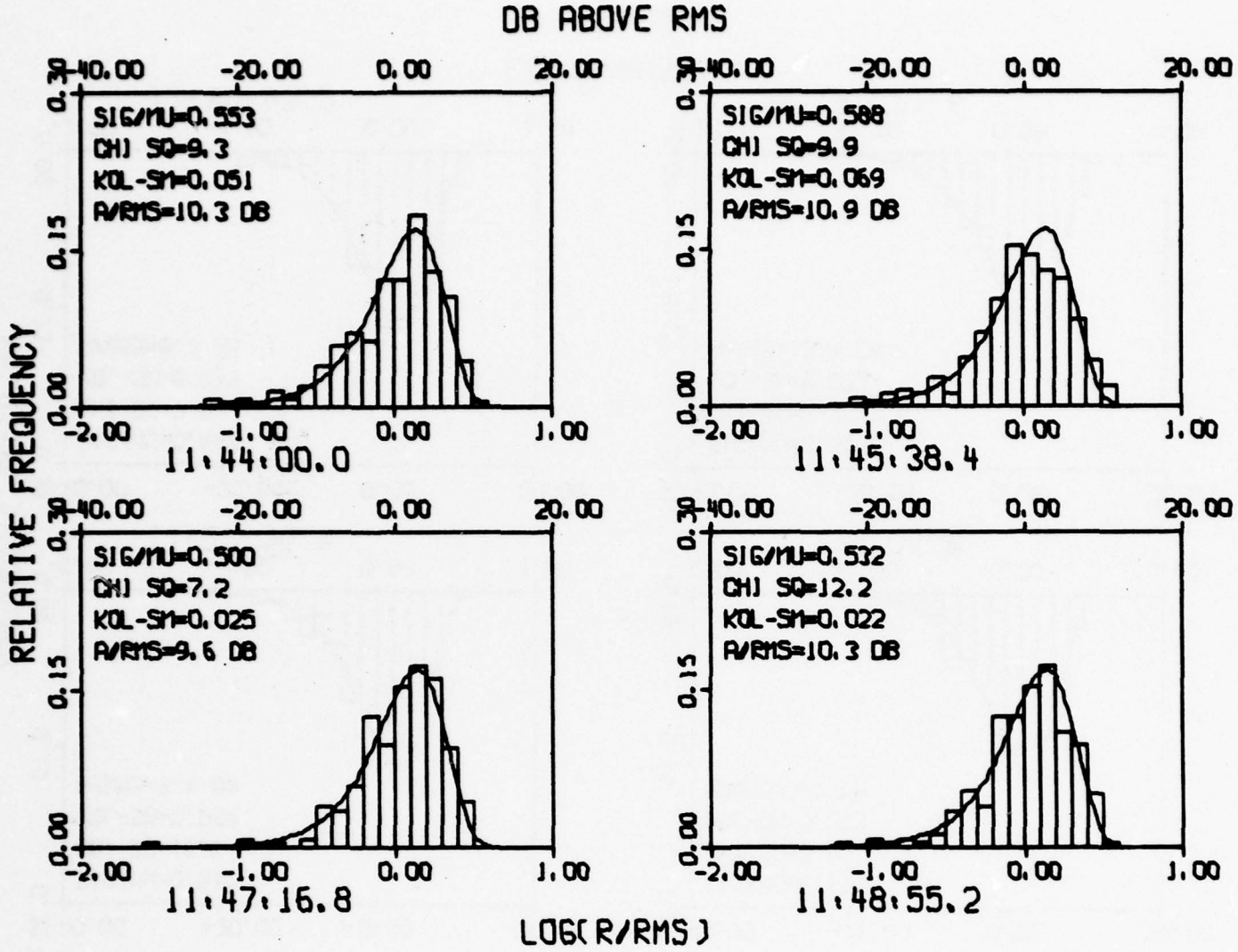

FIGURE III-1

NORMALIZED LOG-ENVELOPE DISTRIBUTIONS FOR SP NOISE, KSRS SITE 1, 9 JUNE 1976
(PAGE 3 OF 10)

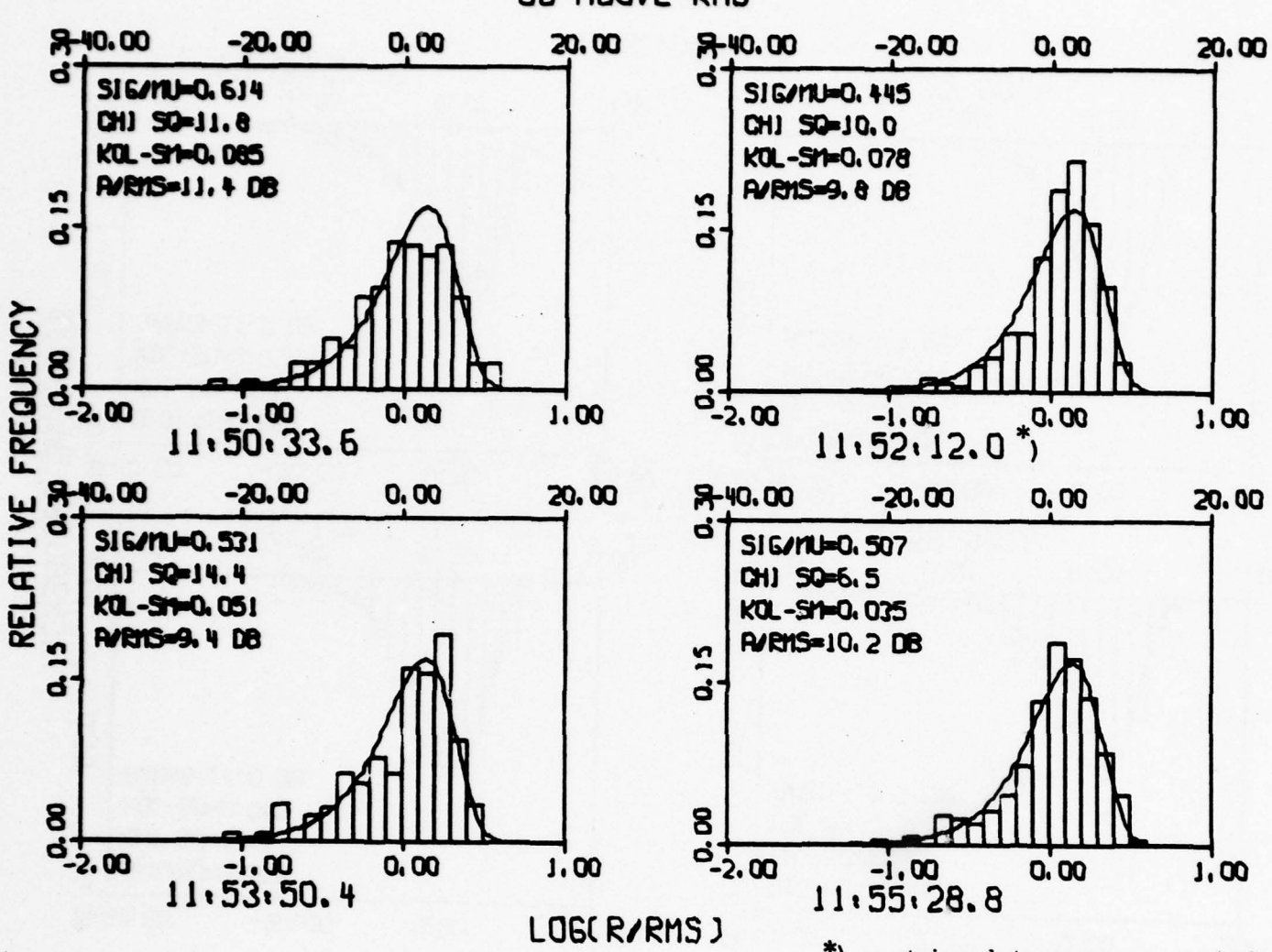

*) contains detector-reported alarm

FIGURE III-1

NORMALIZED LOG-ENVELOPE DISTRIBUTIONS FOR SP NOISE, KSRS SITE 1, 9 JUNE 1976
(PAGE 4 OF 10)

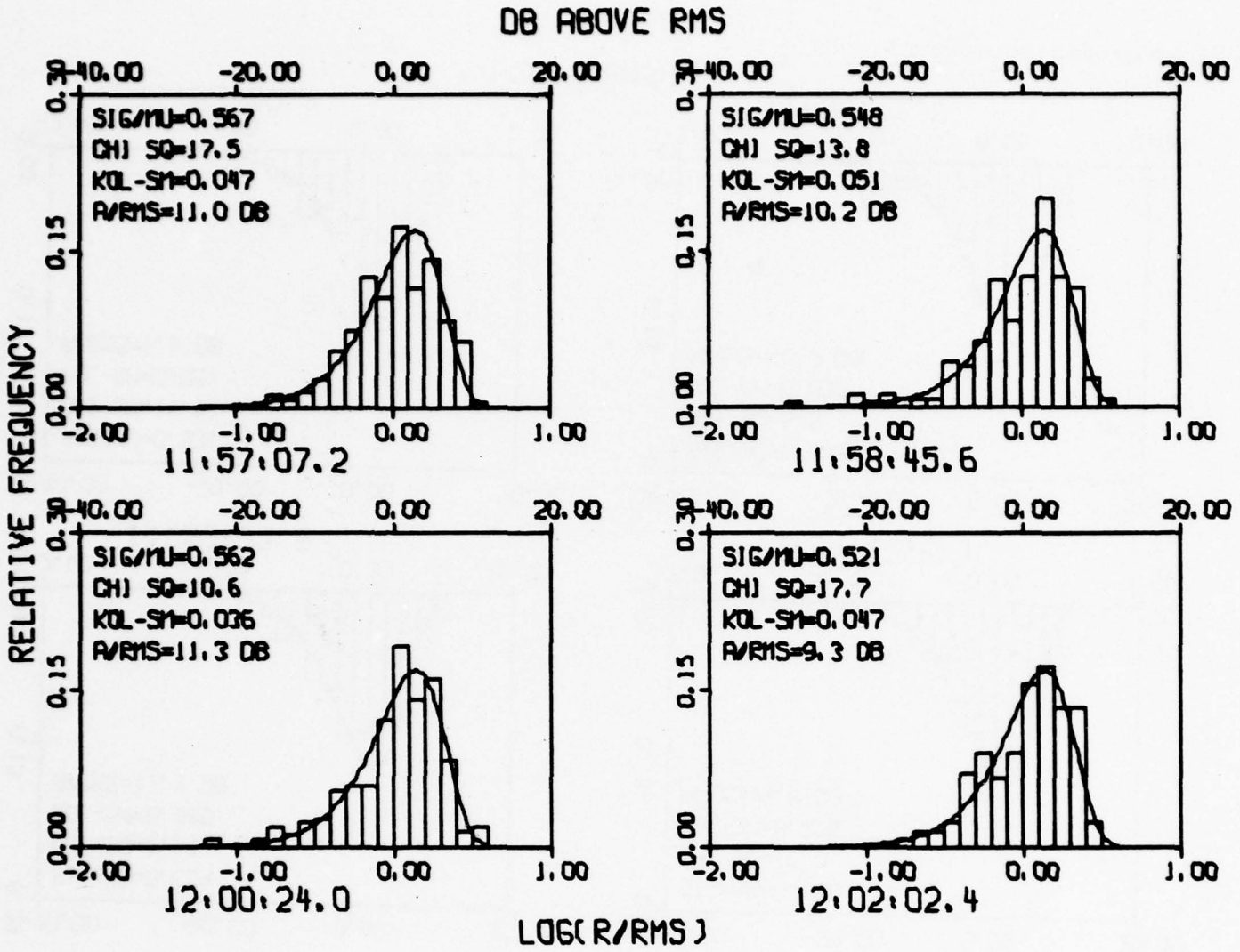

FIGURE III-1

NORMALIZED LOG-ENVELOPE DISTRIBUTIONS FOR SP NOISE, KSRS SITE 1, 9 JUNE 1976

(PAGE 5 OF 10)

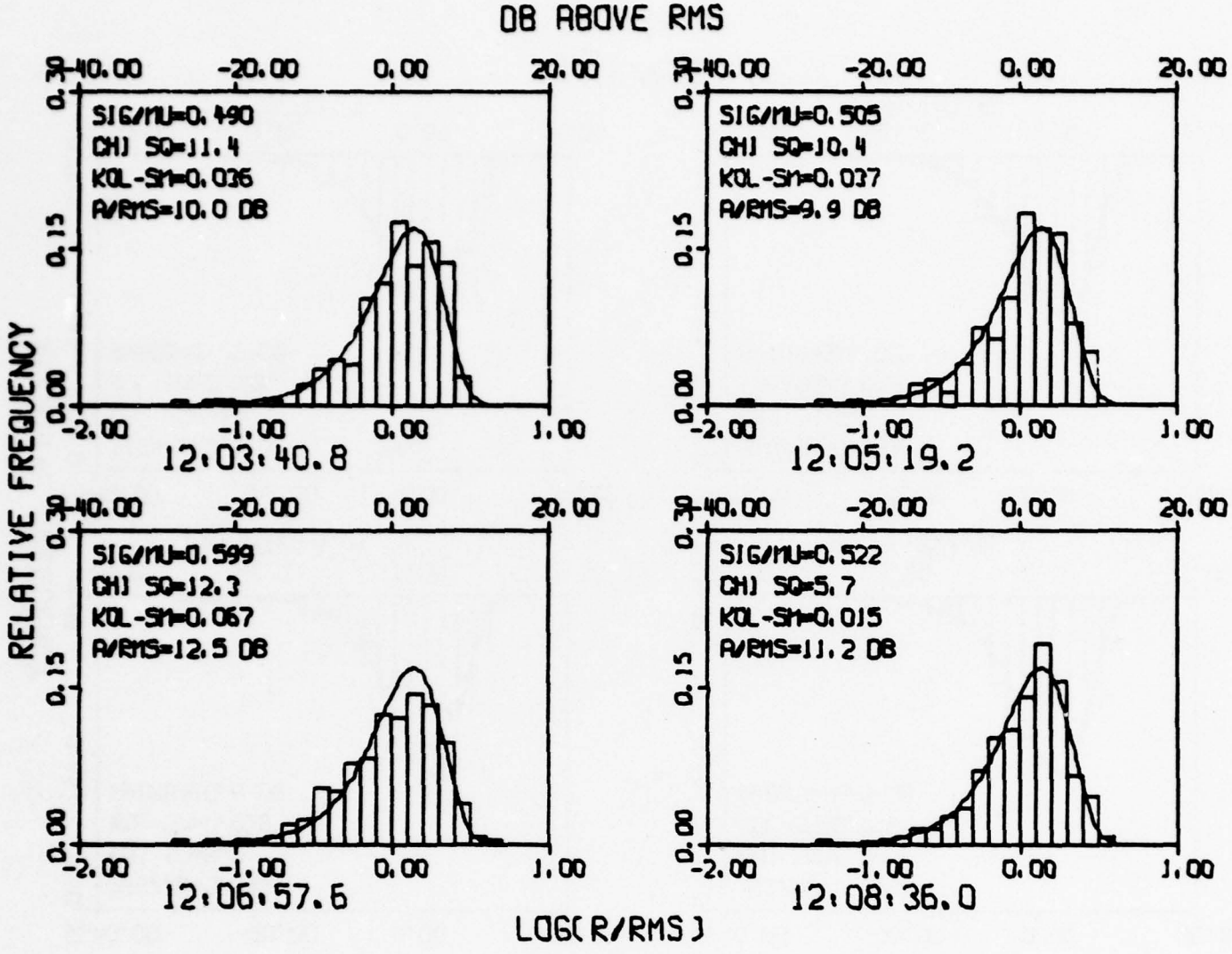

FIGURE III-1

NORMALIZED LOG-ENVELOPE DISTRIBUTIONS FOR SP NOISE, KSRS SITE 1, 9 JUNE 1976
(PAGE 6 OF 10)

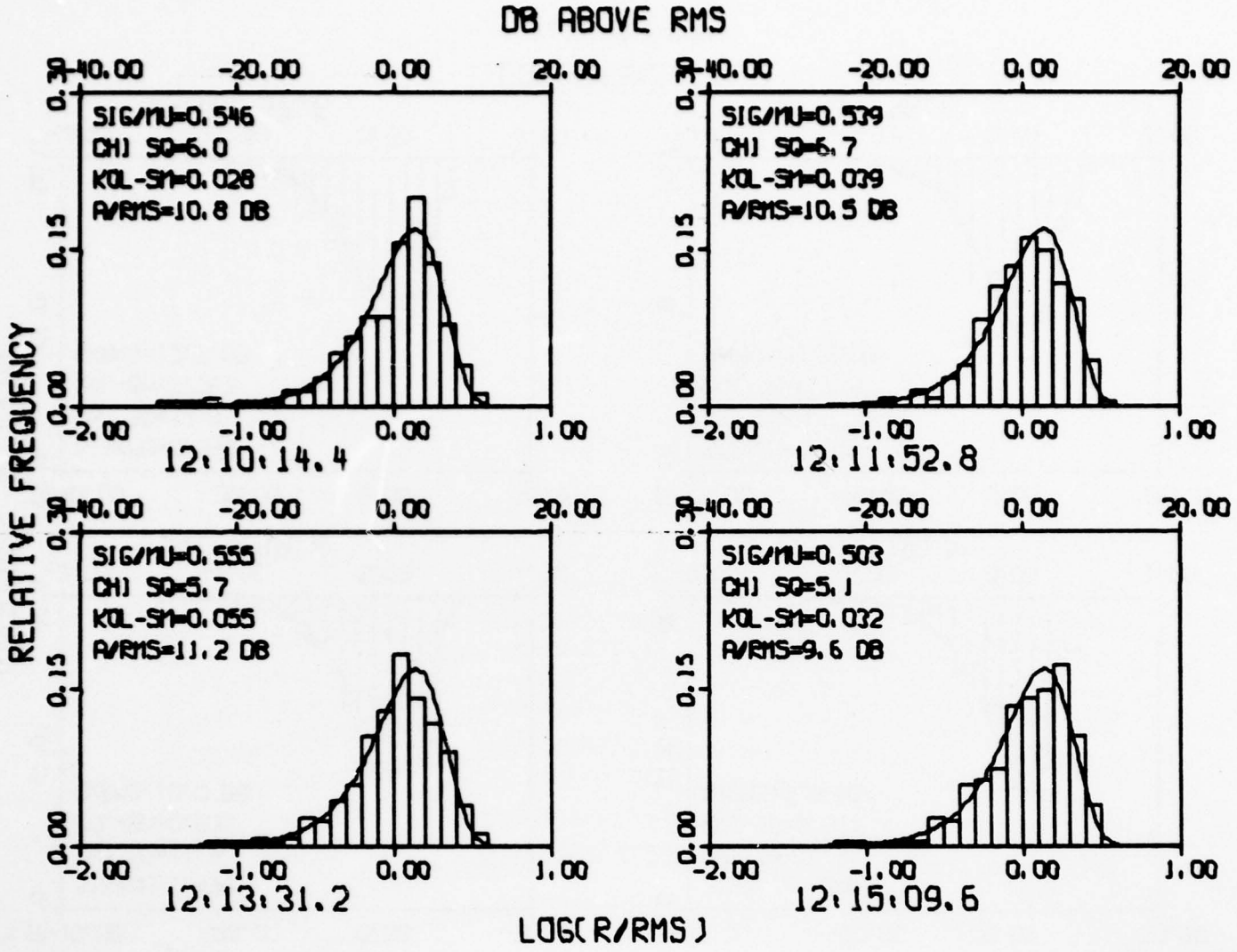

FIGURE III-1

NORMALIZED LOG-ENVELOPE DISTRIBUTIONS FOR SP NOISE, KSRS SITE 1, 9 JUNE 1976
(PAGE 7 OF 10)

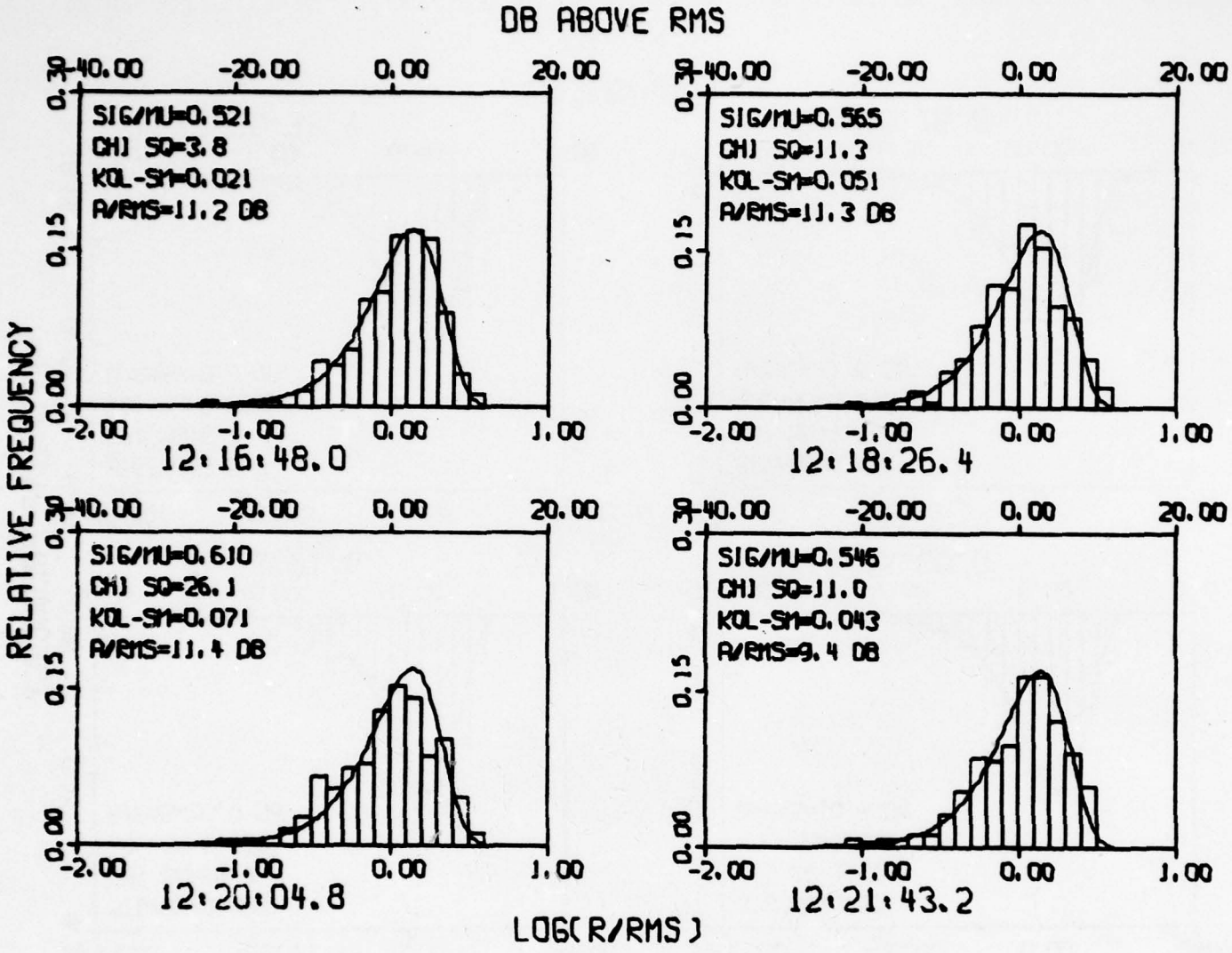

FIGURE III-1

NORMALIZED LOG-ENVELOPE DISTRIBUTIONS FOR SP NOISE, KSRS SITE 1, 9 JUNE 1976
(PAGE 8 OF 10)

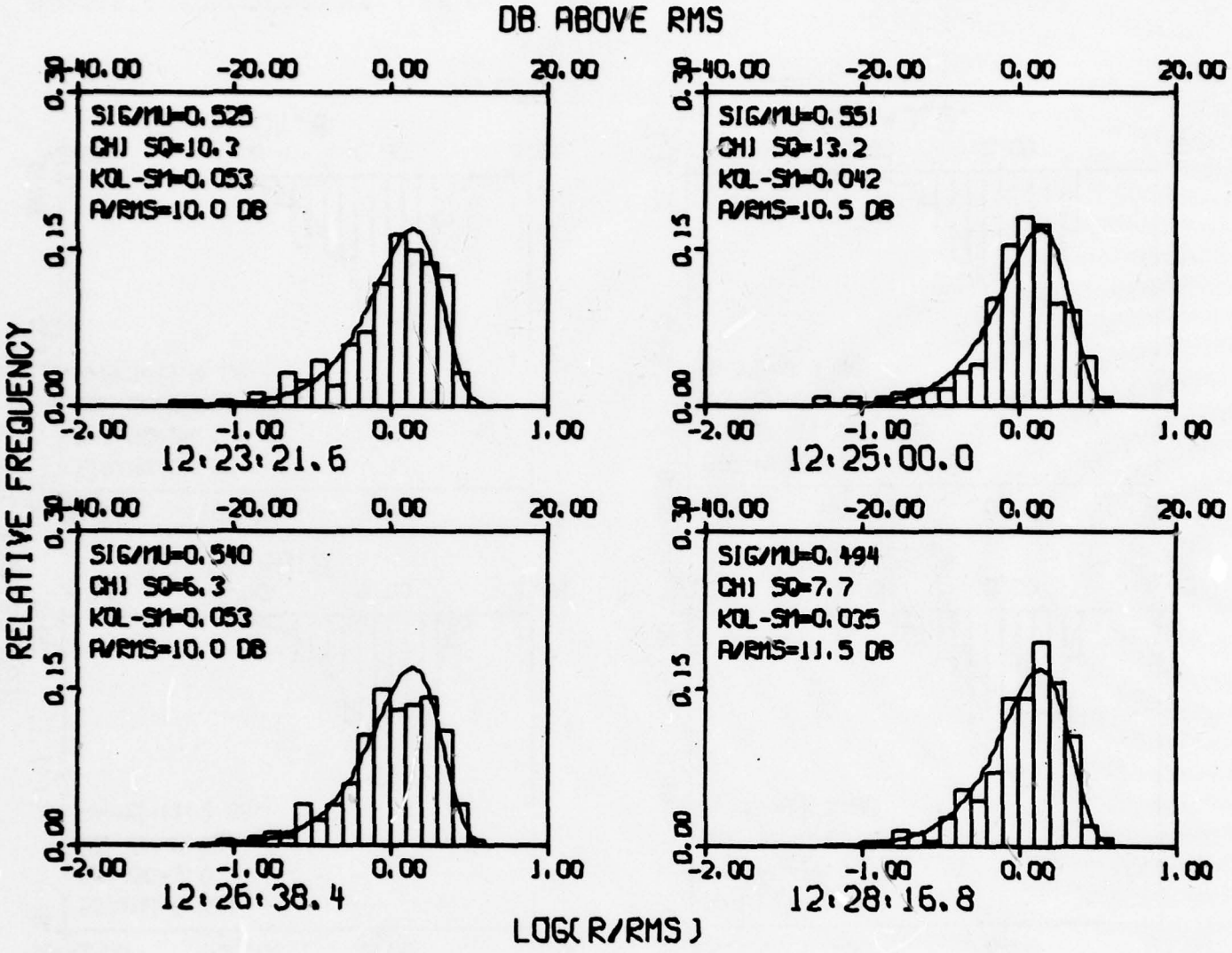

FIGURE III-1

NORMALIZED LOG-ENVELOPE DISTRIBUTIONS FOR SP NOISE, KSRS SITE 1, 9 JUNE 1976
(PAGE 9 OF 10)

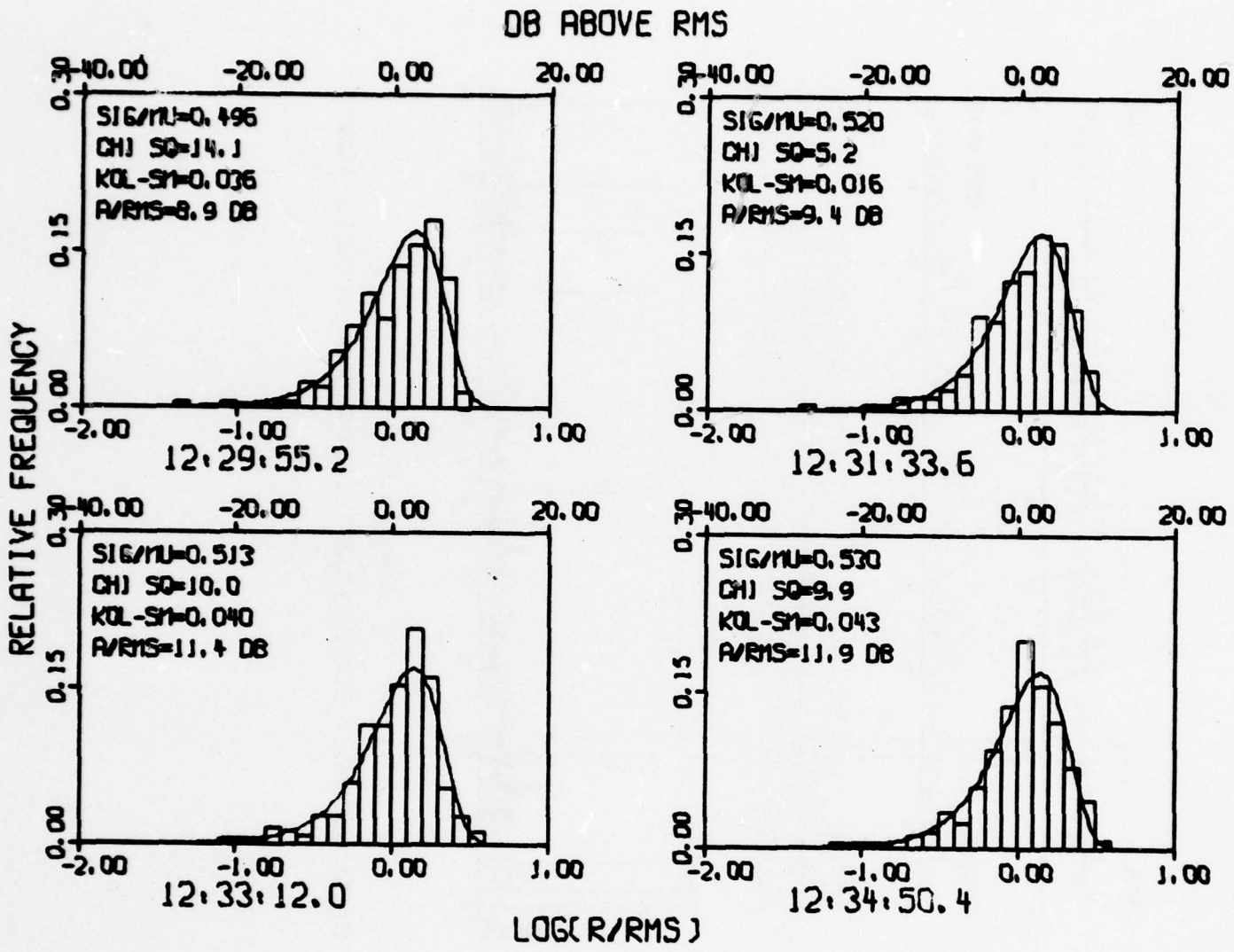

FIGURE III-1

NORMALIZED LOG-ENVELOPE DISTRIBUTIONS FOR SP NOISE, KSRS SITE 1, 9 JUNE 1976
(PAGE 10 OF 10)

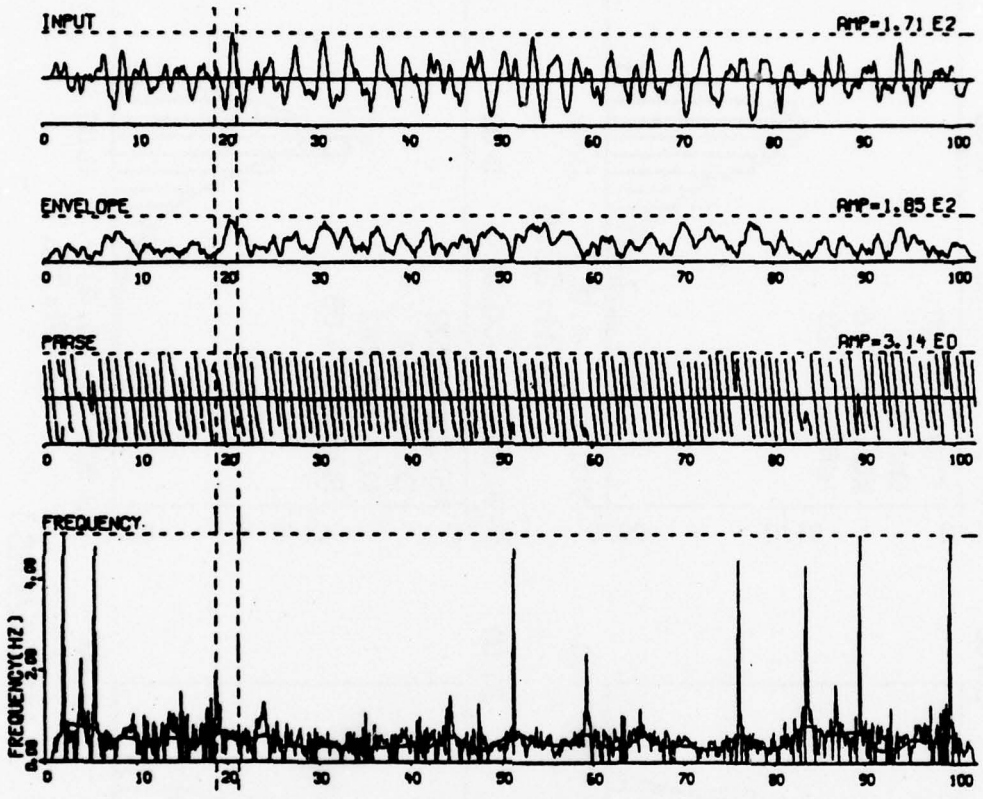

FIGURE III-2

DATA SEGMENT CONTAINING DETECTOR-REPORTED ALARM

Because of the normalization, this theoretical curve is identical in all histograms.

3. Goodness-of-Fit Testing

Four distribution test values are annotated in each histogram. First, the value SIG/MU is the ratio σ_R/μ_R, i.e., the ratio of envelope standard deviation over envelope mean, computed over the entire 102.4-sec data segment. As shown in Section II, for a true Rayleigh distribution, this ratio should equal 0.525, independent of the noise power.

A second test is the chi-square goodness-of-fit test, as described in standard textbooks on statistics (e.g., Lindgren et al., 1978):

$$\chi^2 = \frac{\sum_{i=1}^{k} (f_i - np_i)^2}{np_i} \quad , \qquad \text{(III-2)}$$

where

- k is the number of bins used in the chi-square test,
- f_i is the measured frequency of occurrence in bin i ,
- n is the total number of samples used to compose the histogram, and
- p_i is the hypothetical relative frequency as given by Equation (III-1).

To avoid that the χ^2-values become inflated by low frequency-of-occurrence values in the tails of the distribution, we only use bins in the interval where the theoretical frequency of occurrence is greater than five, as suggested in the literature; i.e., for the values

$$-0.5 \leq y \leq 0.4 \quad , \qquad \text{(III-3)}$$

so that k=10 (9 degrees of freedom). Disadvantages of the chi-square test are:

- The resulting χ^2 distribution depends on the distribution function being tested
- Only part of the distribution is tested.

Especially because of the second item, the chi-square test is not the best one to test a continuous distribution such as our theoretical log-envelope distribution. Yet the χ^2-values were easily computed and, since they should indicate at least a relative goodness-of-fit, they were taken along, and annotated as CHI SQ values in the histograms.

A better test for continuous distributions, according to the literature, is the Kolmogorov-Smirnov goodness-of-fit test:

$$D_n \equiv \max_y \left| F_n(y) - F_o(y) \right| , \qquad \text{(III-4)}$$

where

$F_n(y)$ is the measured cumulative distribution function of the r.v. y , and

$F_o(y)$ is the cumulative distribution function to be tested, i.e., the hypothetical cumulative distribution function.

Thus, D_n equals the maximum absolute deviation between the two cumulative distribution functions. This test has the advantage, that it automatically corrects for the case where the frequency-of-occurrence may not be smoothly distributed over the chosen bins, i.e., if the frequency in one bin is too high, but correspondingly low in the next bin, the Kolmogorov-Smirnov test still will reflect a 'good' fit, whereas the chi-square test will not. Another important advantage is the fact that it is independent of the distribution being tested, and is only a function of the sample size n . The Kolmogorov-Smirnov test values are annotated as KOL-SM values in the histograms.

Finally, we recall our observation in Section II, that the ratio between the maximum envelope value A and the RMS noise value most likely

is 10 to 12 dB for Gaussian noise. This ratio is also annotated in each histogram.

The values of the above test parameters are listed in Table III-2; their distributions are plotted in Figure III-3. The apparent relations among these various test parameters are shown in Figure III-4, in which the values of SIG/MU, CHI SQ and A/RMS, respectively, are plotted against the corresponding KOL-SM values. The ideal SIG/MU value for a Rayleigh distribution of envelopes, and the CHI SQ and KOL-SM 0.05 and 0.20 significance levels α are indicated in both figures. The only 'alarm' reported is indicated with an asterisk.

4. Discussion

Our discussion will be based on how well our theoretical distribution can be used in establishing adequate control of the FAR. We will not discuss the power of the test for retaining the hypothesis that seismic noise is Gaussian. The goodness-of-fit test parameters are given as references for judging the feasibility of using the presumed distribution as a model for FAR control.

As stated earlier, the feasibility of FAR control hinges upon the possibility of obtaining a stationary detection statistic whose distribution can be described, to a good approximation, in closed form. The approximation must be particularly good in the right hand tail of the distribution.

From visual inspection of Figure III-1, we believe that the normalized Gaussian noise model, with the ensuing normalized Rayleigh distribution for normalized noise envelopes, is a reasonably good fit to the observed occurrences, at least for the one-hour KSRS single-site noise sample tested. The normalization process consists of dividing the envelope values by the RMS value of the zero-mean noise seismogram. Thus, to establish adequate FAR control for a given noise frequency band, we merely need to keep a running estimate of the RMS noise value; it does not require averaging of the instantaneous amplitude (envelope) values. Averaging will change the detector's operating characteristics (Section IV).

TABLE III-2

GOODNESS-OF-FIT TEST PARAMETER VALUES

Time	SIG/MU	CHI SQ	KOL-SM	A/RMS (dB)	Time	SIG/MU	CHI SQ	KOL-SM	A/RMS (dB)
11:30:52.8	0.495	6.5	0.035	10.1	12:03:40.8	0.490	11.4	0.036	10.0
11:32:31.2	0.501	5.8	0.019	10.6	12:05:19.2	0.505	10.4	0.037	9.9
11:34:09.6	0.588	14.3	0.075	11.7	12:06:57.6	0.599	12.3	0.067	12.5
11:35:48.0	0.502	6.6	0.024	10.0	12:08:36.0	0.522	5.7	0.015	11.2
11:37:26.4	0.510	15.6	0.048	9.4	12:10:14.4	0.546	6.0	0.028	10.8
11:39:04.8	0.498	7.4	0.033	9.4	12:11:52.8	0.539	6.7	0.039	10.5
11:40:43.2	0.489	7.0	0.027	8.7	12:13:31.2	0.555	5.7	0.055	11.2
11:42:21.6	0.525	6.3	0.023	10.4	12:15:09.6	0.503	5.1	0.032	9.6
11:44:00.0	0.553	9.3	0.051	10.3	12:16:48.0	0.521	3.8	0.021	11.2
11:45:38.4	0.588	9.9	0.068	10.9	12:18:26.4	0.565	11.3	0.051	11.3
11:47:16.8	0.500	7.2	0.025	9.6	12:20:04.8	0.610	26.1	0.071	11.4
11:48:55.2	0.532	12.2	0.022	10.3	12:21:43.2	0.546	11.0	0.043	9.4
11:50:33.6	0.614	11.8	0.085	11.4	12:23:21.6	0.525	10.3	0.053	10.0
11:52:12.0*)	0.445	10.0	0.078	9.8	12:25:00.0	0.551	13.2	0.042	10.5
11:53:50.4	0.531	14.4	0.051	9.4	12:26:38.4	0.540	6.3	0.053	10.0
11:55:28.8	0.507	6.5	0.035	10.2	12:28:16.8	0.494	7.7	0.035	11.5
11:57:07.2	0.568	17.5	0.047	11.0	12:29:55.2	0.496	14.1	0.036	8.9
11:58:45.6	0.548	13.9	0.051	10.2	12:31:33.6	0.520	5.2	0.016	9.4
12:00:24.0	0.562	10.6	0.036	11.3	12:33:12.0	0.513	10.0	0.040	11.4
12:02:02.4	0.521	17.7	0.047	9.3	12:34:50.4	0.530	9.9	0.043	11.9

*) contains detector-reported 'alarm'

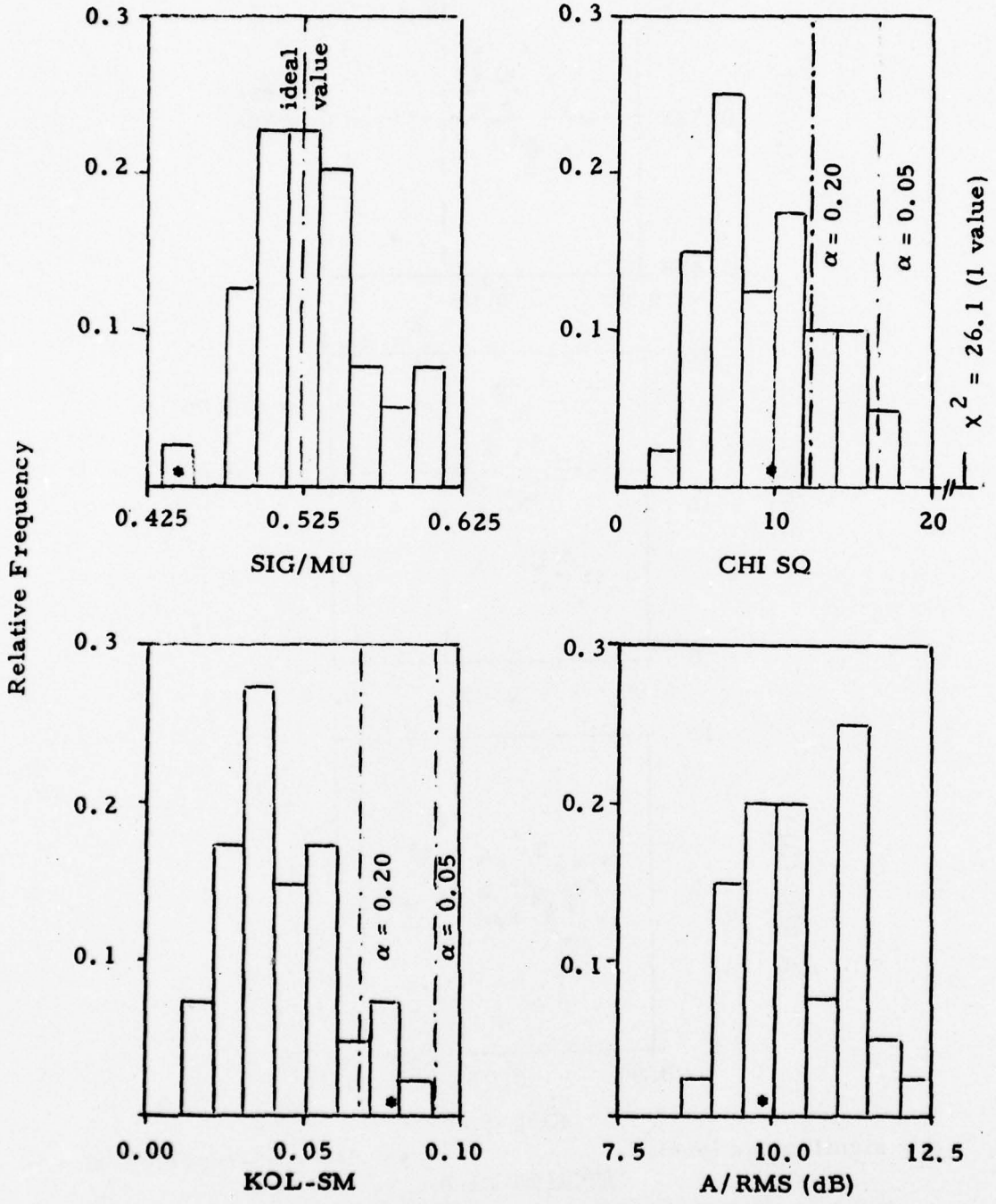

α = significance level; • = detector-reported 'alarm'

FIGURE III-3

DISTRIBUTIONS OF GOODNESS-OF-FIT TEST PARAMETER VALUES

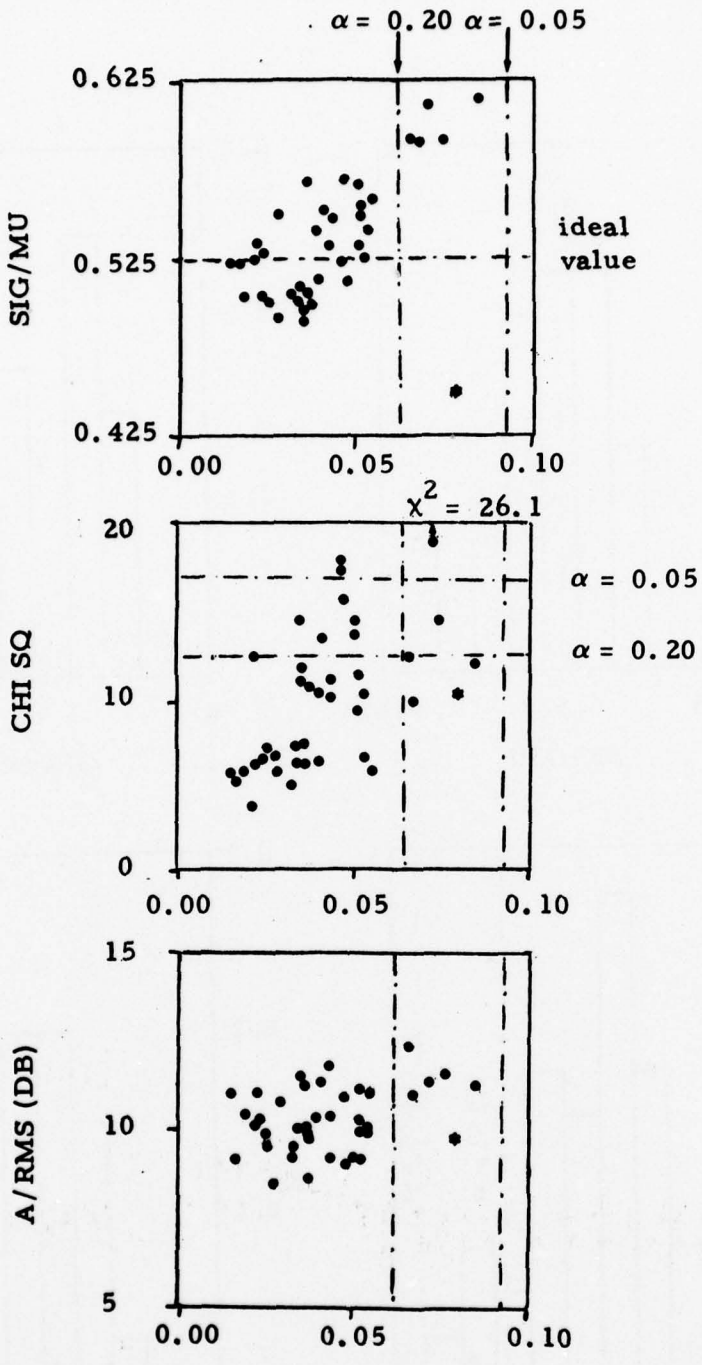

α = significance level; * = detector-reported 'alarm'

FIGURE III-4

TEST PARAMETER RELATIONSHIPS

In 80% of the cases, the hypothetical distribution correctly describes at least the right hand tail of the empirical envelope distributions; there, the theoretical curve goes virtually through the bin centers at the corresponding relative frequency of occurrence. Exceptions are listed in Table III-3, with the test parameters repeated from Table III-2. It includes an evaluation of the difference in FAR these tail discrepancies could cause if we would set a threshold at 11 dB above RMS. The remarks in Table III-3 describe the major feature of the particular tail discrepancy. For thresholds of 12 dB or higher there would not be an increase in the FAR, except at 12:06:57.6 (Figure III-1) where a value of 12.5 dB above RMS was recorded. The value of 0.4 extra false alarms listed in Table III-3 for this case is based on 102.4 sec of data. As we see in Figure III-1, no other histogram shows envelope values above 12 dB above RMS in the entire one-hour data segment, suggesting a FAR of only 0.4 FA/H for a single detection trial at a threshold of 12 dB above RMS.

Considering Figures III-3 and III-4, we note first that the tabulated significance levels correspond fairly well with the cumulative relative frequencies, i.e., 15% of the Kolmogorov-Smirnov test values, and 22.5% of the chi-square test values are greater than the respective 20% significance levels. Second, it seems that the SIG/MU values start to diverge beyond the KOL-SM 20% significance level. Third, besides the extreme value $\chi^2 = 26.1$, only one other test value falls beyond the KOL-SM/ CHI SQ 20% joint significance level. Fourth, there seems to be adequate correlation between CHI SQ and KOL-SM test values, but the spread in this relationship increases considerably with increasing test values. Finally, we observe that of the envelope distributions with tail discrepancies listed in Table III-3, either the CHI SQ or the KOL-SM test values are near or above the 20% significance level.

The waveforms and the envelope, phase and frequency time traces of two data segments, one with a very good fit and another with a poor fit, are displayed in Figure III-5. Besides some difference in waveform character

TABLE III-3

ENVELOPE DISTRIBUTIONS WITH DEVIATING TAIL

Time	SIG/MU	CHISQ	KOL-SM	A/RMS	ΔFA*)	Remarks
11:34:09.6	0.588	14.3	0.075	11.7	0.9	bin-quantization noise
11:45:38.4	0.588	9.9	0.069	10.9	1.8	visually non-Rayleigh
11:50:33.6	0.614	11.8	0.085	11.4	2.1	visually non-Rayleigh
12:00:24.0	0.562	10.6	0.036	11.3	1.4	bin-quantization noise
12:06:57.6	0.599	12.3	0.067	12.5	0.4	large A/RMS value
12:18:26.4	0.565	11.3	0.051	11.3	1.4	non-Rayleigh?
12:29:55.2	0.496	14.1	0.036	8.9	--	FAR overestimation
Total expected FAR deviation:					8.0 FA/H = 20%**)	

*) Number of false alarms above theoretical number (= 1.1) for 102.4-sec data segment, assuming 0.36-sec independent-sample interval and envelope threshold of 11 dB above RMS noise; single detection trial.

**) Number of false alarms, for one-hour KSRS noise sample, above theoretical FAR (= 40 FA/H) for 11 dB threshold; single envelope detection trials.

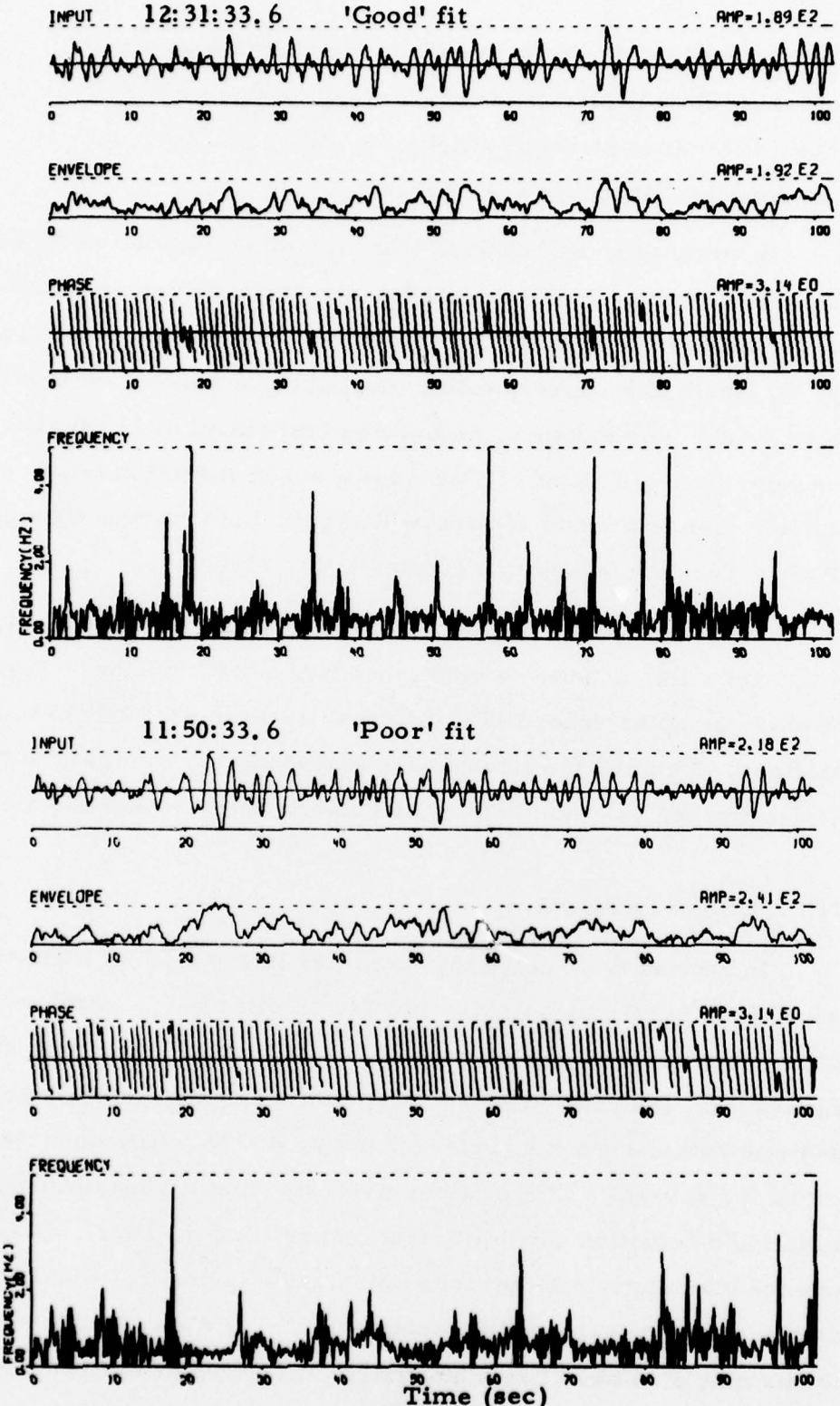

FIGURE III-5

DATA SEGMENTS WITH GOOD AND POOR FIT, RESPECTIVELY, TO GAUSSIAN NOISE MODEL

there is little to suggest that the poor-fit waveform contains a signal. The same was observed for all data segments in the one-hour KSRS noise sample. Neither did any of the instantaneous amplitude, phase and frequency traces display any anomalies; all looked very similar.

In summary, we conclude that, for this one-hour KSRS noise sample, the Gaussian noise model is an adequate model to use as a basis for FAR control in envelope detection. For a desired FAR, we only need to set the envelope threshold at a corresponding level above a running estimate of the RMS noise level. For instance, an envelope threshold of 12 dB above the RMS noise should yield a FAR of 13 FA/H for a single detection trial. Employing multiple detection trials and additional detection criteria can strongly reduce this FAR. We will discuss this further in Section IV.

These analytical results should be tested with at least 24 hours of noise data. They also need to be confirmed with noise envelope distribution analysis on noise samples recorded at different times of day and year, and at different stations. Finally, the interval for independent sampling of a waveform needs to be determined as a function of the noise frequency band (Section IV).

C. OTHER OBSERVATIONS

In Section II we noted that the most likely ratio of maximum-envelope-over-RMS for Gaussian noise is 10 to 12 dB. D. G. Lambert observed that in noise waveforms recorded at stations of the Very Long Period Experiment (VLPE), the ratio between maximum noise amplitudes and RMS noise values was rather constant (Lambert et al., 1973). This observation was confirmed for several VLPE stations when studying the feasibility to determine a station's detection capability from noise (Unger, 1974). See Table III-4. Since the maximum instantaneous noise value in general equals the maximum noise envelope value within about one dB, this suggests that those LP waveforms may also have Rayleigh-distributed envelopes and, therefore,

TABLE III-4

AVERAGE MAXIMUM-AMPLITUDE-OVER-RMS RATIOS FOR VLPE NOISE*)

Station	Acro-nym	AA/RMS	s.d.	A/RMS (dB)	No. Noise samples**
Charter Towers, Australia	CTA	8.61	2.14	12.7	26
Chiang Mai, Thailand	CHG	7.34	1.20	11.3	31
Kongsberg, Norway	KON	6.55	0.58	10.3	32
Kipapa, Hawaii	KIP	6.73	0.80	10.5	48
Albuquerque, New Mexico	ALQ	6.26	0.36	9.9	30
La Paz, Bolivia	ZLP	6.60	0.68	10.4	21

*) Unger (1974), p. III-11

**) AA = largest peak-to-peak amplitude in one-hour noise sample

A = largest peak amplitude in one-hour noise sample

s.d. = standard deviation of AA/RMS measurements

would stem from a truly Gaussian noise process. Although all A/RMS values in Table III-4 agree with those for Gaussian noise, those for CTA and CHG are larger and have considerably greater variances than those for KON, KIP, ALQ, and ZLP. This may suggest that noise at the latter stations is more closely Gaussian than that at CTA and CHG.

We furthermore remark that in many cases, based on empirical observations, a 10 dB peak-over-RMS ratio is accepted by analysts as a standard value for noise waveforms.

D. POWER DATA

Since our main interest in this study is in envelope statistics, no special effort was made to collect distributions of the instantaneous power. However, Swindell and Snell (1977) collected data for short-term averages (STA) of the instantaneous power in order to obtain a Gaussian detection statistic. Some of their results are shown in Figure III-6, presenting distributions for logSTA - logLTA values obtained with 0.8, 1.6, and 3.2-sec STA averaging times. LogLTA is the long-term (1 to 2 min) mean of the logSTA values, so that LTA approximately equals the long-term average of the noise power, and is comparable to the total power N or RMS^2 in our previous analyses. The distributions were compiled from two hours of uninterrupted KSRS beam noise; in our present study we used the first hour of this same period to compile our KSRS single-site envelope distributions.

As observed by the authors, the distribution is more skewed for the shorter integration times. The distribution for the 0.8-sec integration time takes on more the shape of the instantaneous power distribution given in Figure II-6. Note in particular the fact that the most likely value occurs near 0 dB, consistent with our derivations. This helps to explain why a zero-mean, near-Gaussian statistic is obtained by averaging just a few independent samples of instantaneous power (four 0.4-sec samples for the 1.6-sec gate; eight for the

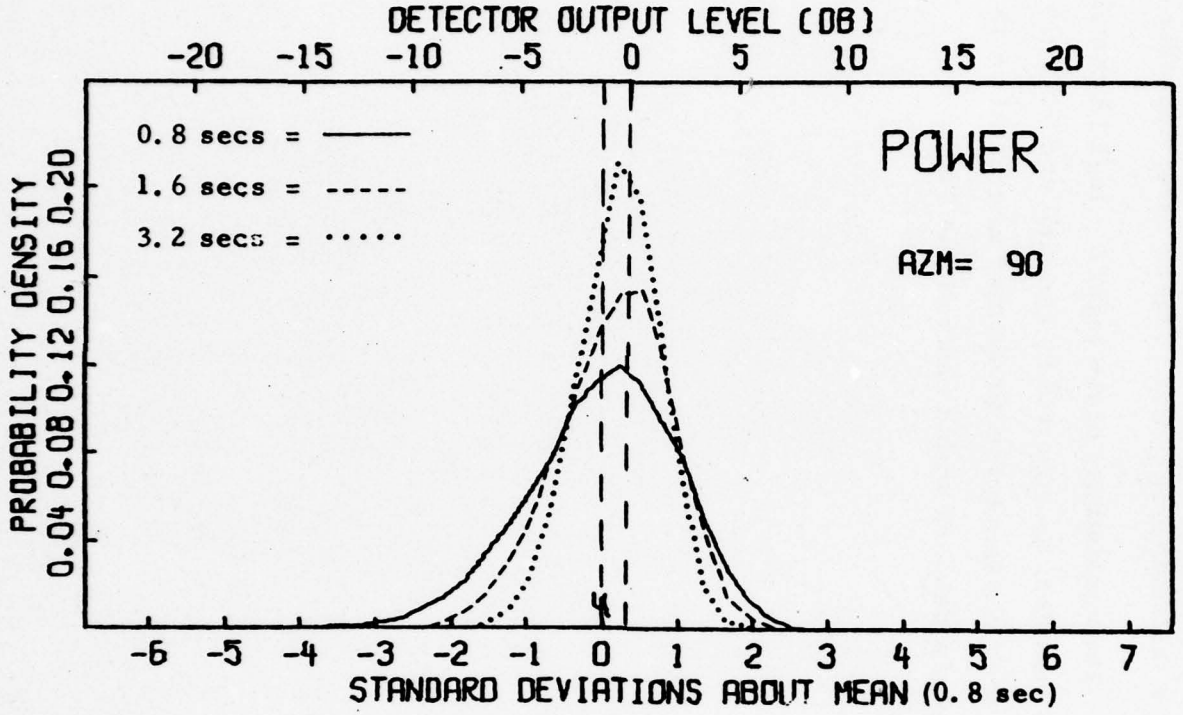

FIGURE III-6

DISTRIBUTIONS OF LOG(STA) - LOG(LTA), FOR VARIOUS AVERAGING TIMES. KSRS 90° BEAM, 9 JUNE 1976, 11:30-13:30 (SWINDELL AND SNELL, 1977; p. III-10)

3.2-sec gate). As reported by the authors, the means of these distributions occur slightly different from 0 dB due to the fact that the instantaneous power is first averaged before the base-ten logarithm is taken, rather than averaging the logarithms of the instantaneous power. This difference approximately equals $0.215\ (\sigma_p/\mu_p)^2$, where σ_p and μ_p are the standard deviation and the mean of the instantaneous power (Unger, 1974; Appendix C).

The consistency of the logSTA - logLTA distributions over various noise samples, as reported by Swindell and Snell (1977), strongly suggests that the Gaussian noise model may in general be an adequate basis for the design of a detector with a controllable FAR.

SECTION IV
DETECTOR DESIGN CONSIDERATIONS

A. INTRODUCTION

In the previous two sections we have shown that the Gaussian noise model, which generates waveforms whose envelopes follow the Rayleigh distribution, provides a stationary detection statistic for which adequate control of the FAR can be derived. Below, we will discuss briefly a number of ways to best use the information obtained. The underlying feature of all design strategies is the assumption that a certain tolerable false alarm rate will be imposed through a surveillance system's threshold control (Sax et al., 1974; Unger et al., 1974). For the given FAR, the probability of detection then needs to be maximized. This is basically the Neyman-Pearson decision rule, treated in the classical decision theory and applied by various authors to the field of communications technology (Selin, 1965; Schwartz et al., 1966; Van Trees, 1968).

To discuss these design strategies in great detail is beyond the scope of our present task. Our discussion merely serves to suggest various approaches that may be taken, and to indicate areas requiring further research, in the process of optimizing the design for a front-end SP signal detector. For more details the reader is referred to the above mentioned literature.

B. SIGNAL DETECTION BY GOODNESS-OF-FIT TESTING

The results obtained in Section III in testing the goodness-of-fit of the envelope Rayleigh distribution suggest that the test values SIG/MU, CHI SQ, KOL-SM, and possibly A/RMS, may be used to either retain or reject

the null hypothesis of the Gaussian noise model. Rejection of this null hypothesis at a certain significance level α , corresponding to a desired FAR, then would imply the presence of a signal.

Such a procedure would require continuous updating of the normalized envelope distribution. The normalization process requires a running estimate of the RMS noise level. For this strategy it is extremely important to determine the minimum interval between independent samples, and the minimum number of samples (the shortest possible gate) from which a valid noise envelope distribution may be estimated. Furthermore, the effect of signals on the envelope distribution must be investigated; the distribution of signal-plus-noise envelopes will determine the decision 'power' of the test, i.e., the probability of detection, P_D. In particular, we would like to know if a relatively weak signal would effect the total noise distribution to an extent that the null hypothesis can be rejected at a specified significance level.

As a final remark on this strategy, it must be realized that any form of sufficiently non-Gaussian noise would be recognized as 'signal'. Such false alarms may be due to large noise fluctuation from cultural sources, atmospheric disturbances, or distributed ocean sources. Given a detection, the analyst must perform additional waveform analysis to determine if the detection satisfies the definition of a 'signal' as it is to be processed in a surveillance system, i.e., in detection association, event location and classification, etc. Too many 'detections' of non-Gaussian noise could cause the FAR to exceed a level required for optimum execution of the above seismic network functions.

C. SIGNAL DETECTION BY LIKELIHOOD RATIO TESTING

In many signal detection cases the optimum test is a likelihood ratio test (LRT). Let $p_1(y)$ and $p_0(y)$ be the probability density functions of a r.v. y under the condition that a signal is present or absent, respectively.

The LRT then consists of forming the likelihood ratio

$$L(y) = \frac{p_1(y)}{p_0(y)} \quad , \tag{IV-1}$$

comparing L(y) with a threshold K, and deciding

D_0 (only noise present) if $L \leq K$,

D_1 (signal + noise present) if $L > K$.

Under the Neyman-Pearson decision rule the choice of K depends on the tolerable FAR.

For m multiple observations or detection trials $\underline{y} = y_1, y_2, \ldots, y_m$, the likelihood ratio is the ratio of the joint probability density functions:

$$L(\underline{y}) = \frac{p_1(y_1, y_2, \ldots, y_m)}{p_0(y_1, y_2, \ldots, y_m)} \quad . \tag{IV-2}$$

If the observations are independent this becomes

$$L(\underline{y}) = \frac{\prod_{i=1}^{m} p_1(y_i)}{\prod_{i=1}^{m} p_0(y_i)} \quad . \tag{IV-3}$$

In many cases the distributions p_1 and p_0 contain exponential factors, some of which may be common to both distributions. Cancelling the common factors, and taking natural logarithms on both sides of Equation (IV-3) usually reduces the likelihood ratio to a relatively simple detection statistic which maximizes P_D for given $P_F = \alpha$. For instance, in the case of envelope detection of a signal with constant amplitude in Gaussian noise by multiple-observation, likelihood ratio testing, the optimum necessary and sufficient

detection statistic can be shown to be the mean-square envelope for low SNR and the envelope mean for high SNR (Schwartz et al., 1966). This test is uniformly most powerful in the sense that it is independent of either the SNR or the signal amplitude; any other test for this case would be less powerful. The power of the test, i.e., P_D, increases with both, the SNR and the number of independent observations. One can also say that the test is optimum in the sense that, for given P_D and P_F, it minimizes the SNR required for signal detection. Typically, every doubling of the number of independent observations (up to a certain limit) lowers the required SNR by about 3 dB (Schwartz et al., 1966).

In the case of seismic event signal detection, however, there are various factors which may make it difficult to perform an optimum test in the above fashion. First, the number of independent observations is a function of signal duration and of signal frequency which, in turn, depend on type, magnitude, and orientation of the seismic event and on the propagation characteristics. Second, in general we deal with signals which have certain rise and decay times. Also, especially in the case of most nuclear explosions, there is constructive and destructive interference caused by early arriving multiple signals. The signal amplitude, therefore, is far from constant, and optimizing the test for this case is a difficult task, requiring further analysis.

These problems are recognized in radar technology as 'fading'. Several techniques have been developed to cope with this problem (Schwartz et al., 1966; part III). Among these are diverse space, time and frequency sampling of the signal waveform. These techniques also hold promise in seismic event signal detection. For instance, since fading will frequently be different at different sites of a seismic array, appropriate multichannel signal processing may improve the detection of fading signals. In time diversity, repetitions of the signal transmission serve a similar function. In frequency diversity, finally, a bank of narrowband filters could be employed, and outputs

combined, under the assumption that the fading would vary in different frequency bands.

D. AN ANALYST-TYPE DETECTION MODEL

We will now turn to the envelope detector designed recently (Unger, 1978) and attempt to evaluate its features based on the information from Sections II and III. This detector, designed to closely follow the detection logic usually applied by an analyst, operates on two detection criteria (also mentioned in Section II) which must be satisfied simultaneously:

- The signal-plus-noise envelope, sampled within a test gate of given length, must exceed the maximum lagging noise envelope for a specified percentage of the total number of samples (e.g., for 30%, or twelve 0.1-sec samples, in a 4-sec test gate).
- The ratio between the first 'signal-plus-noise' envelope peak in the test gate and the long-term maximum noise envelope must exceed a given value (e.g., 2 or 3 dB).

Furthermore, the maximum noise envelope test value is forced to decay with time. This enables the detector to follow long-term (1 to 2 min) noise level variations.

The expected number of times that, in a T-sec test gate, in the absence of signal, the envelope exceeds the lagging, long-term maximum noise envelope A is

$$M = \frac{T}{\Delta T} \cdot P_F(A/RMS) \quad , \qquad \text{(IV-4)}$$

where ΔT is the interval between independent samples and P_F is the probability of a false alarm of a single detection trial, as derived in Section II for normalized envelopes of a Gaussian noise process. In Table IV-1 we list a

TABLE IV-1

EXPECTED NUMBER OF TIMES THAT NOISE ENVELOPE IN 4-SEC TEST GATE EXCEEDS LONG-TERM MAXIMUM NOISE ENVELOPE A, FOR GIVEN A/RMS*)

A/RMS (dB)	P_F **)	M ***)
12	1.34×10^{-3}	1.34×10^{-2}
10	1.69×10^{-2}	1.69×10^{-1}
8	7.88×10^{-2}	7.88×10^{-1}

*) Assuming 0.4-sec independent-sample interval

**) From Table II-1

***) From Equation (IV-4)

number of M-values as a function of A/RMS values, assuming $T = 4$ sec and $\Delta T = 0.4$ sec, and using the P_F-values listed in Table II-1. In evaluating the envelope detector (Unger, 1978) we used threshold values of 10% and 30% for the first detection criterion. For $T = 4$ sec and $\Delta T = 0.4$ sec, this corresponds to $M = 1$ and $M = 3$, respectively. In view of Table IV-1 these values seem quite reasonable. Only in the unlikely case that high noise envelopes are clustered within a narrow time interval would a false alarm be generated. In contrast, for signals, we expect that relatively high envelopes are sustained over at least a relatively short interval. It is this contrast which enhances the power of our hypothesis testing, or, equivalently, the probability of detection.

We will now focus on the second criterion. The probability that a noise peak in the test gate exceeds the lagging long-term noise peak A by B dB is

$$P_B = 1 - \left(1-P_F(y_{A,B})\right)^{T/\Delta T} , \qquad \text{(IV-5)}$$

where

$$y_{A,B} = \log A/RMS + B/20 . \qquad \text{(IV-6)}$$

For instance, according to Table IV-1, if A/RMS = 10 dB, a SNR threshold of B = 2 dB would result in a probability of 0.0132 that, in the absence of signal, the long-term noise peak is exceeded by 2 dB by the noise peak envelope in the test gate.

We realize from the above considerations that the events of noise satisfying each criterion individually are not independent. The joint probability of noise satisfying both criteria simultaneously, therefore, must be less than each of the individual probabilities but greater than their product. Thus, denoting the probability of noise satisfying the first criterion by P_C, we

have

$$P_B \cdot P_C < P_{BC} < \min(P_B, P_C) \quad . \tag{IV-7}$$

This shows a range over which the second criterion further reduces the false alarm rate for this detector.

Clearly, for a given pair of threshold settings, the false alarm rate of our detector depends on the fluctuation of noise peak-to-RMS ratios. Although this ratio was observed to be relatively constant, its fluctuation occurs over a range where the probability of false alarm increases rather sharply with decreasing A/RMS as evidenced by Tables II-1 and IV-1. This may cause some instability in the detector's FAR. The extent of this instability is difficult to assess analytically; based in part on preliminary empirical evaluation, the FAR will probably fluctuate between 0.1 and 10 FA/H for threshold settings of 30% and 3 dB for the respective detection criteria.

This FAR stability may be judged unsatisfactory for control of a seismic surveillance system. For Gaussian noise, the FAR can be stabilized by referencing our envelope detection criteria to the RMS noise level rather than to the maximum noise envelope.

Such an envelope detection algorithm resembles that of an STA/LTA type detector. The essential differences between the envelope and the STA/LTA type detectors lie in the choice, the normalization procedure, and the further employment of the detection statistic. These differences are summarized in Table IV-2, for the automatic Seismic Research Observatory (SRO) detector, the automatic power detector designed by Swindell and Snell (1977), and the above suggested envelope detection scheme. The latter is attractive in the sense that, in the case of Gaussian noise, and employing single detection trials, stable FAR control requires neither short-term averaging of the

TABLE IV-2

BASIC FEATURES OF RELATED DETECTORS

Detector	Detection Statistic	Normalization Procedure
SRO *)	STA of rectified instantaneous value.	STA/LTA
Power **)	STA of instantaneous power.	$\frac{\text{logSTA} - \mu_{\text{logSTA}}}{\sigma_{\text{logSTA}}}$
Envelope ***)	Instantaneous amplitude, R(t). No STA. Multiple, independent detection trials. Multiple detection criteria.	log (R/RMS) or R/RMS

STA is the short-term (1 to 4 seconds) average

LTA is the long-term (1 to 2 minutes) average

*) Eterno et al. (1974); Strauss and Weltman (1977)

**) Swindell and Snell (1977)

***) Unger (1978), with suggested envelope normalization

instantaneous detection statistic, nor dividing by the standard deviation. As pointed out previously, employing an instantaneous detection statistic enables multiple detection trials within a presumed signal gate, which can considerably improve the detector operating characteristics.

This improvement, however, depends on the number of independent samples available in the test gate. This number is determined by the noise spectrum. Variation in the noise spectrum, therefore, may cause some instability in the FAR. For instance, the interval between independent samples is 0.4 sec for a bandwidth of 2.5 Hz, 0.5 sec for 2.0 Hz. Thus, for a 4-sec test gate, a change from 2.5 to 2.0 Hz in the noise bandwidth would change the number of independent trials from 10 to 8, and increase the FAR accordingly. It may be feasible to obtain a stable FAR for this envelope detector, by making the threshold dependent on the noise bandwidth. The above also suggests that the use of multiple filters with partially overlapping bandwidths may benefit the detector's operating characteristics. These issues need further evaluation.

Further improvements of an analyst-type detection model by expanding the number of detection observables were proposed previously (Unger, 1978). These observables could include the envelope slope, the instantaneous phase, and the instantaneous frequency. The distribution of these parameters under noise-only conditions need to be determined before the feasibility of their incorporation can be assessed.

Together with the initial evaluation results obtained with the envelope detector in its present stage, the above indicates that it should be feasible to design, if necessary by slight modification of the present algorithm, an envelope detector with a controllable FAR, operating, for instance, at 1 FA/H for approximately 80% signal detection. This projection, of course, must be confirmed with extended empirical evaluation. Further experimentation with the threshold controls may lead to further improvement of the

operating characteristics. For fading signals, such as those from seismic events, we believe that the present envelope detector with the proposed modifications will have near-optimum operating characteristics.

As seen in Section III, for the purpose of FAR control, the Gaussian noise hypothesis can be retained at a significance level of 5% or possibly less. Most likely, this will cover a great number of seismic station noise conditions; this needs to be verified empirically. For conditions under which the Gaussian noise hypothesis has to be rejected at this relatively low significance level, the stability and the predictability of the FAR for a given threshold setting may become questionable. Even under these conditions, however, we expect that the analyst-type envelope detector model, operating with multiple detection trials and multiple detection criteria relative to the long-term maximum envelope, will provide close to the best possible performance characteristics.

E. STA/LTA-TYPE DETECTOR MODELS

Above, we mentioned briefly both the apparent similarity and the essential differences between the envelope detector and two kinds of STA/LTA-type detectors. The experience gained with employment of the latter may be useful in the design of an envelope detector. In our previous analyses, we already discussed some of this experience. Below, we will elaborate on the FAR stability of STA/LTA-type detectors.

In Section II we found that, for Gaussian noise, the normalized instantaneous power and the normalized instantaneous amplitude are stationary detection statistics. The same can possibly be derived for a normalized version of the rectified instantaneous value. The normalization process consists of dividing the instantaneous detection parameter by a long-term average: the long-term average noise power for power detection, the long-term RMS noise for envelope detection. We would not expect that taking a short-term average

would change the stationary character of the normalized detection statistic. For Gaussian noise, therefore, we would expect that straight STA/LTA detectors have a constant FAR for a given threshold setting. However, straight STA/LTA detectors have been reported to suffer from FAR instability (Lacoss, 1972; Steinert et al., 1975; Swindell and Snell, 1977). This instability must be caused by either of two conditions, or a combination of these:

- The STA is non-stationary
- The noise is non-Gaussian.

In the case of Gaussian noise, a non-stationary STA statistic may arise when the noise spectrum is non-stationary; the number of independent samples of an instantaneous detection parameter within a waveform gate of given length then would vary with time. Since the variance of the STA depends on the number of independent samples in the test gate, noise spectrum variation would lead to fluctuation in the STA variance. This makes the STA a non-stationary detection statistic, causing FAR instability. For this case, the FAR of STA/LTA detectors can be stabilized by normalizing the STA statistic not only relative to the noise power level (the LTA), but also with respect to the STA variance. This method was suggested by Lacoss (1972), and implemented by Swindell and Snell (1977) in their design of an automatic power detector with a constant FAR.

Since averaging a r.v. will tend to make it Gaussian, the above process may also work well in the case of non-Gaussian noise. In particular, the logarithm of the STA of the instantaneous power becomes near-Gaussian for relatively short averaging times (Lacoss, 1972; Swindell and Snell, 1977; see also Sections II and III of this report).

Finally, we remark that averaging of an instantaneous detection statistic in certain cases is equivalent to performing a likelihood ratio test, which may be an optimum test for those cases (Section II).

The difference in performance between a detector employing short-term averaging with proper STA normalization, and a detector operating with multiple detection trials and multiple detection criteria, should be further investigated.

F. DETECTOR-REPORTED ALARM

The envelope detector in its present design stage (Unger, 1978), with the adaptations and operating parameters as described in Section III, was applied to the one-hour KSRS single-site noise sample analyzed in this study. The detector reported one alarm for this one-hour period. Below we will analyze this alarm in terms of the test parameters described in Section III.

The reported alarm occurred at 11:53:16.3, in the data segment starting at 11:52:12.0. The log-envelope distribution for this segment is shown on page 4 of Figure III-1; the waveforms are presented in Figure III-2. The goodness-of-fit test parameters for this segment are marked with an asterisk in Table III-2, and in Figures III-3 and III-4.

We note that, although the right hand tail of this data segment's envelope distribution fits the Rayleigh distribution very well, the relative frequencies to the left of, and including the most likely value, show considerable deviation. This is also evidenced by the extreme SIG/MU value, the high KOL-SM value, and, to a lesser extent, by the CHI SQ value. As observed for the waveforms of other data segments with unfavorable test values, however, there is little indication of signal presence in Figure III-2, suggesting that this was a false alarm.

SECTION V
SUMMARY

Distributions of the base-ten logarithm of instantaneous amplitude (envelope) values from one hour of uninterrupted, unfiltered KSRS single-site, SP noise were analyzed. The one-hour noise sample was divided into 102.4-sec data segments. Taking 0.4-sec envelope samples, the log-envelope distribution was compiled for each data segment, in 2 dB bins. The evaluation led to the following conclusions:

- For the envelopes of this one-hour noise sample the Rayleigh distribution, which is the theoretical envelope distribution for waveforms generated by a Gaussian noise process, can be retained at the Kolmogorov-Smirnov 5% significance level.
- Given a Rayleigh distribution, a stationary, normalized detection statistic is obtained by dividing the envelope values by a long-term (1 to 2 minutes) running estimate of the RMS noise distribution.
- At the 5% significance level of retention, the Rayleigh distribution seems an adequate model for deriving stable control of the FAR of an envelope detector. For a single detection trial, a tolerable false alarm rate can be maintained merely by setting the envelope signal detection threshold at a corresponding level above the RMS noise level. For instance, a threshold setting of 12 dB above RMS should yield 13 false alarms per hour. This is yet to be confirmed empirically.

- Employing multiple, independent detection trials and multiple detection criteria can further reduce the false alarm rate. The amount of false alarm rate reduction depends on the noise frequency band. Therefore, noise frequency variation may cause some false alarm rate instability. The optimum operating parameters will have to be determined empirically.

- For Rayleigh-distributed envelopes in an approximately 1.5-minute gate, the theoretically most likely value of the ratio between the maximum noise envelope or the maximum instantaneous noise value, and the RMS noise level is 10 to 12 dB. This value is routinely observed by seismogram analysts. Since for Gaussian noise this ratio is nearly constant, a detector operating relative to the long-term noise envelope maximum, e.g., with a threshold of 3 dB above this maximum, may have a near-constant false alarm rate. It may exhibit a relatively stable performance also under non-Gaussian noise conditions.

- A recently developed envelope detector (Unger, 1978) operating relative to the long-term noise envelope maximum, and using multiple detection trials and multiple detection criteria closely following an analyst's detection logic, reported one false alarm over the one-hour noise sample. Determination of reliable operating characteristics for this detector model requires further empirical evaluation.

- A detection statistic need not be Gaussian in order to enable efficient false alarm rate control; it merely has to be stationary. Parameters derived from a Gaussian process can conveniently be transformed into stationary detection statistics. Examples are normalization of the Rayleigh-distributed envelope and normalization of the instantaneous power.

- In view of the above, in the case of Gaussian noise, taking a short-term average (STA) of an instantaneous detection statistic is not mandatory in the design of a controlled false alarm rate detector. In fact, fluctuations in the noise frequency band would cause the STA statistic to be non-stationary (Lacoss, 1972; Steinert et al., 1975); this explains the reported false alarm rate instability in straight STA/LTA detectors. The STA/LTA false alarm rate can be stabilized by proper normalization of the STA statistic (Lacoss, 1972; Swindell and Snell, 1977).

- Short-term averaging, followed by STA normalization, may enhance the detector operating characteristics in the sense of performing a likelihood ratio test for multiple trials or observations in the detection of signals of constant amplitude. It also may provide a means of controlling the false alarm rate for non-Gaussian noise.

- For signals of non-constant amplitude, such as most seismic signals, it is difficult to analytically optimize the detector design. A combination of analytical and empirical evaluation seems necessary. In particular, the strategy of normalized STA/LTA detection (e.g., Swindell and Snell, 1977) should be compared to that of employing multiple, independent detection trials and multiple detection criteria based on instantaneous detection statistics (Unger, 1978).

- For all possible detector design strategies, it is extremely important to determine the shortest interval between independent samples as a function of the noise frequency band.

- The suggested noise model should be tested on noise data recorded at different times of day and year, and at a variety of

stations. Sufficiently long detector runs should be carried out to establish the validity of the noise model in predicting the occurrences of noise alarms in the tail of the distribution, i. e., at false alarm rates sufficiently low for optimum network operation.

SECTION VI
REFERENCES

Eterno, J. S., D. S. Burns, L. J. Freier, and S. W. Buck, 1974; Special Event Detection for an Unattended Seismic Observatory; Report No. R-765, ARPA Contract Number F44620-73-C-0057, The Charles Stark Draper Laboratory, Incorporated, Cambridge, MA.

Lacoss, R. T., 1972; Variation of False Alarm Rates of NORSAR, Semi-annual Technical Summary, Seismic Discrimination, Massachusetts Institute of Technology, Cambridge, MA, June, 53-72.

Lambert, D. G., S. R. Prahl, and A. C. Strauss, 1973; Evaluation of the Noise Characteristics and the Detection and Discrimination Capabilities of the Very Long-Period Experiment (VLPE) Single Stations and the VLPE Network, Special Report No. 14, Texas Instruments Report No. ALEX(01)-STR-73-14, AFTAC Contract Number F33657-72-C-0725, Texas Instruments Incorporated, Dallas, TX.

Lindgren, B. W., G. W. McElrath, and D. A. Berry, 1978; Introduction to Probability and Statistics, MacMillan Publishing Company, Inc., New York, NY.

Prahl, S. R., W. W. Shen, and R. L. Whitelaw, 1975; Preliminary Evaluation of the Korean Seismological Research Station Short-Period Array, Technical Report No. 5, Texas Instruments Report No. ALEX(01)-TR-75-05, AFTAC Contract Number F08606-75-C-0029, Texas Instruments Incorporated, Dallas, TX.

Sax, R. L., 1965; Stationarity of Seismic Noise, Geophysics, 4, 668-674.

Sax, R. L., and staff, 1974; Seismic Network Systems Study, Special Report No. 17, Texas Instruments Report No. ALEX(01)-STR-74-01, AFTAC Contract Number F33657-72-C-0725, Texas Instruments Incorporated, Dallas, TX.

Sax, R. L., and Technical Staff, 1978; Event Identification-Applications to Area of Interest Events, Technical Report No. 20, Texas Instruments Report No. ALEX(01)-TR-78-08, AFTAC Contract Number F08606-77-C-0004, Texas Instruments Incorporated, Dallas, TX.

Schwartz, M., W. R. Bennett, and S. Stein, 1966; Communication Systems and Techniques, McGraw Hill, Inc., New York, NY.

Selin, I., 1965; Detection Theory, Princeton University Press, Princeton, NJ.

Shen, W. W., 1977; Study of Adaptive Beamforming Algorithms for Low Magnitude Seismic P-Wave Detection, Technical Report No. 5, Texas Instruments Report No. ALEX(01)-TR-77-05, AFTAC Contract Number F08606-77-C-0004, Texas Instruments Incorporated, Dallas, TX.

Shen, W. W., 1978; Detection Performance of Time-Varying Adaptation Rate Adaptive Beamformer, Technical Report No. 18, Texas Instruments Report No. ALEX(01)-TR-78-06, AFTAC Contract Number F08606-77-C-0004, Texas Instruments Incorporated, Dallas, TX.

Steinert, O., S. Husebye, and H. Gjøystdal, 1975; Noise Variance Fluctuations and Earthquake Detectability, J. Geophys. 41, 289-302.

Strauss, A. C., and L. C. Weltman, 1977; Continuation of the Seismic Research Observatories Evaluation, Technical Report No. 2, Texas Instruments Report No. ALEX(01)-TR-77-02, AFTAC Contract Number F08606-77-C-0004, Texas Instruments Incorporated, Dallas, TX.

Swindell, W. H., and N. S. Snell, 1977; Station Processor Automatic Signal Detection System, Phase I: Final Report, Station Processor Software Development; Texas Instruments Report No. ALEX(01)-FR-77-01, AFTAC Contract Number F08606-76-C-0025, Texas Instruments Incorporated, Dallas, TX.

Unger, R., 1974; Estimating a Seismic Station's Detection Capability from Noise, Application to VLPE Stations, Technical Report No. 4, Texas Instruments Report No. ALEX(01)-TR-74-04, AFTAC Contract Number F08606-74-C-0033, Texas Instruments Incorporated, Dallas, TX.

Unger, R., 1978; Automatic Detection, Timing and Preliminary Discrimination of Seismic Signals with the Instantaneous Amplitude, Phase and Frequency, Technical Report No. 4, Texas Instruments Report No. ALEX (01)-TR-77-04, AFTAC Contract Number F08606-77-C-0004, Texas Instruments Incorporated, Dallas, TX.

Unger, R., S. S. Lane, and R. L. Sax, 1974; Aspects of Information Feedback and Parameter Update Design for a Seismic Surveillance System, Technical Report No. 14, Texas Instruments Report No. ALEX(01)-TR-74-14, AFTAC Contract Number F08606-74-C-0033, Texas Instruments Incorporated, Dallas, TX.

Van Trees, H. L., 1968; Detection, Estimation, and Modulation Theory, Part I, John Wiley and Sons, Inc., New York, NY.